Electronic Supplementary Material (ESI) for CrystEngComm.

Supplementary Information

Steric crowding of a series of pyridine based ligands influencing the photophysical properties of Zn(II) complexes

Daniel Ejarque [a], *Teresa Calvet* [b], *Mercè Font-Bardia* [c], *and Josefina Pons* [a,*]

[a]Departament de Química, Universitat Autònoma de Barcelona, 08193-Bellaterra, Barcelona, Spain

[b]Departament de Mineralogia, Petrologia i Geologia Aplicada, Universitat de Barcelona, Martí i Franquès s/n, 08028 Barcelona, Spain

[c]Unitat de Difracció de Raig-X, Centres Científics i Tecnològics de la Universitat de Barcelona (CCiTUB), Universitat de Barcelona, Solé i Sabarís, 1-3, 08028 Barcelona, Spain

*Corresponding author E-mail: josefina.pons@uab.es

FTIR-ATR, ^{1}H, $^{13}C\{^{1}H\}$ and DEPT-135 NMR spectroscopies

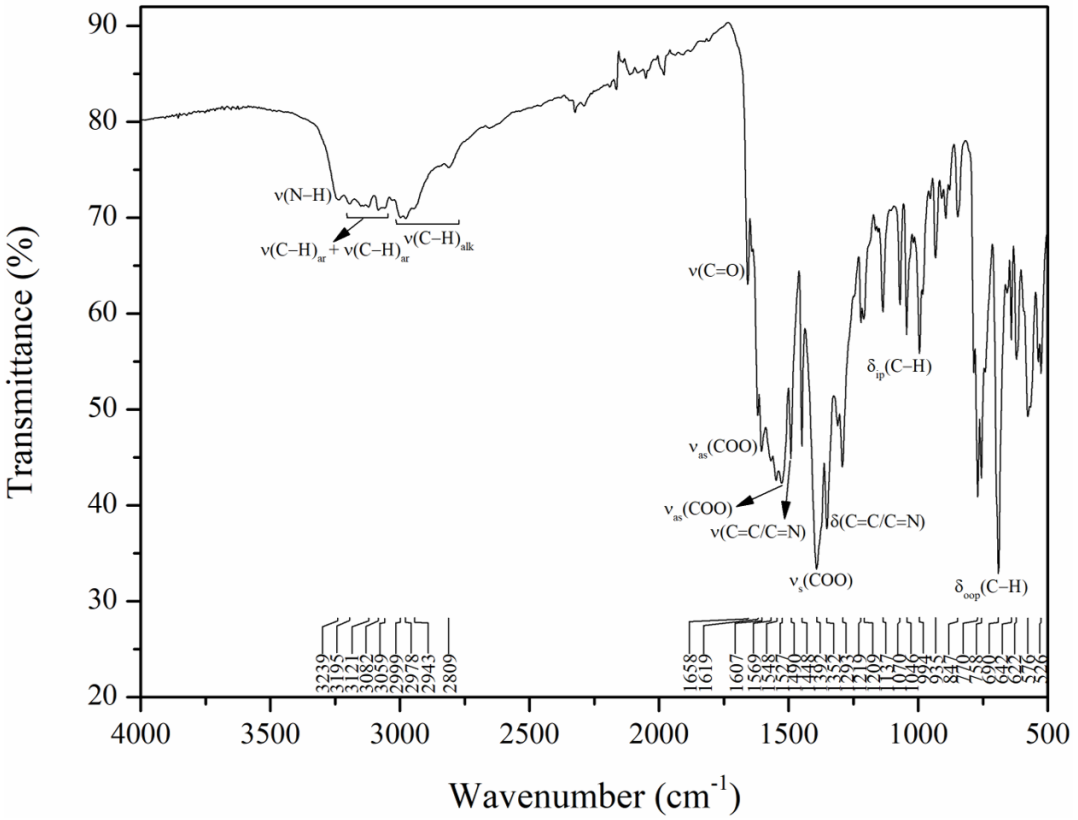

Figure S1. FTIR-ATR spectrum of compound $[Zn(\mu\text{-}O,O'\text{-}ACA)(ACA)(py)]_n$ (**1**).

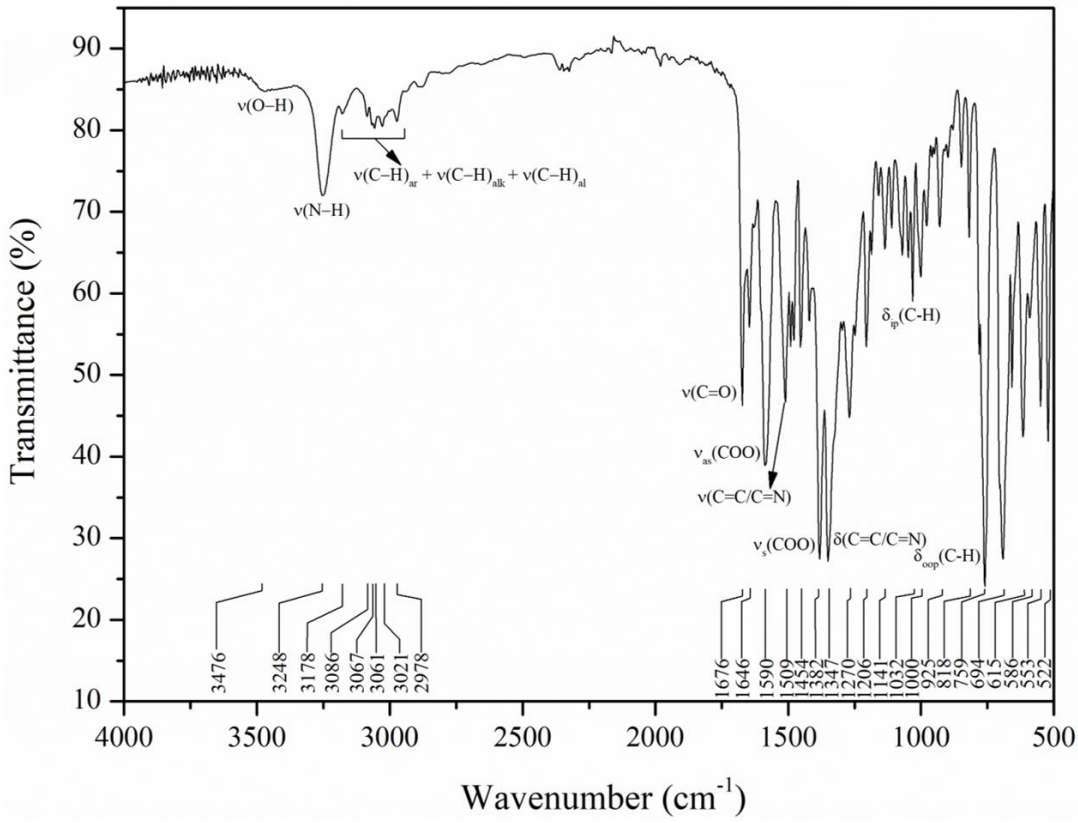

Figure S2. FTIR-ATR spectrum of compound $[Zn(ACA)_2(3\text{-}phpy)_2]\cdot EtOH$ (**2**).

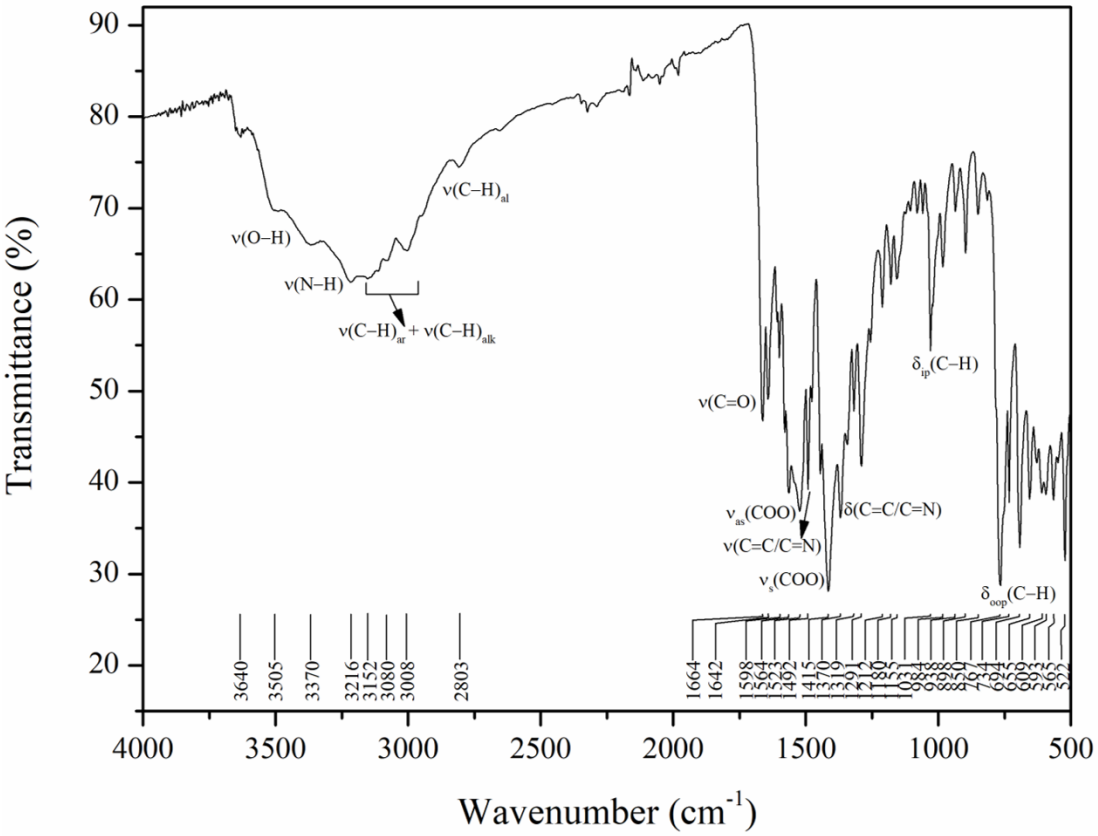

Figure S3. FTIR-ATR spectrum of compound [Zn(ACA)$_2$(2,2'-bipy)]·4EtOH (**3**).

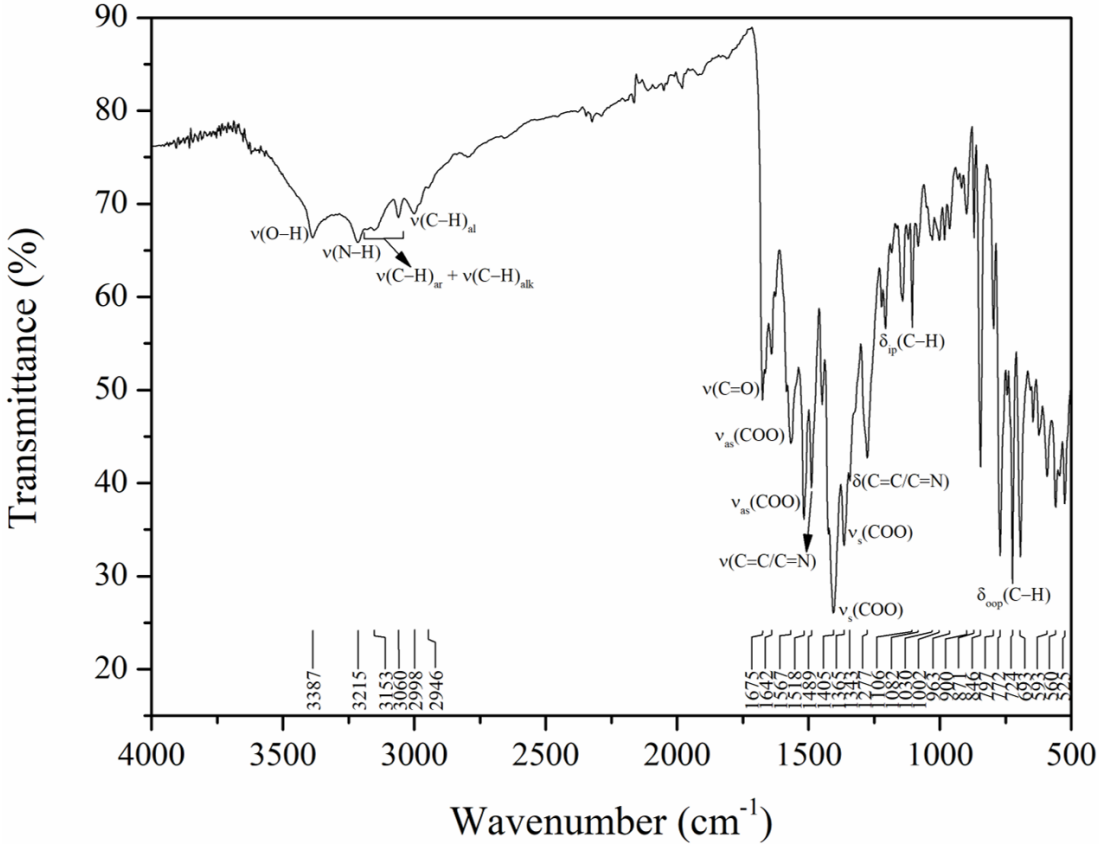

Figure S4. FTIR-ATR spectrum of compound [Zn(ACA)$_2$(1,10-phen)][Zn(ACA)$_2$(1,10-phen)]·3EtOH (**4**).

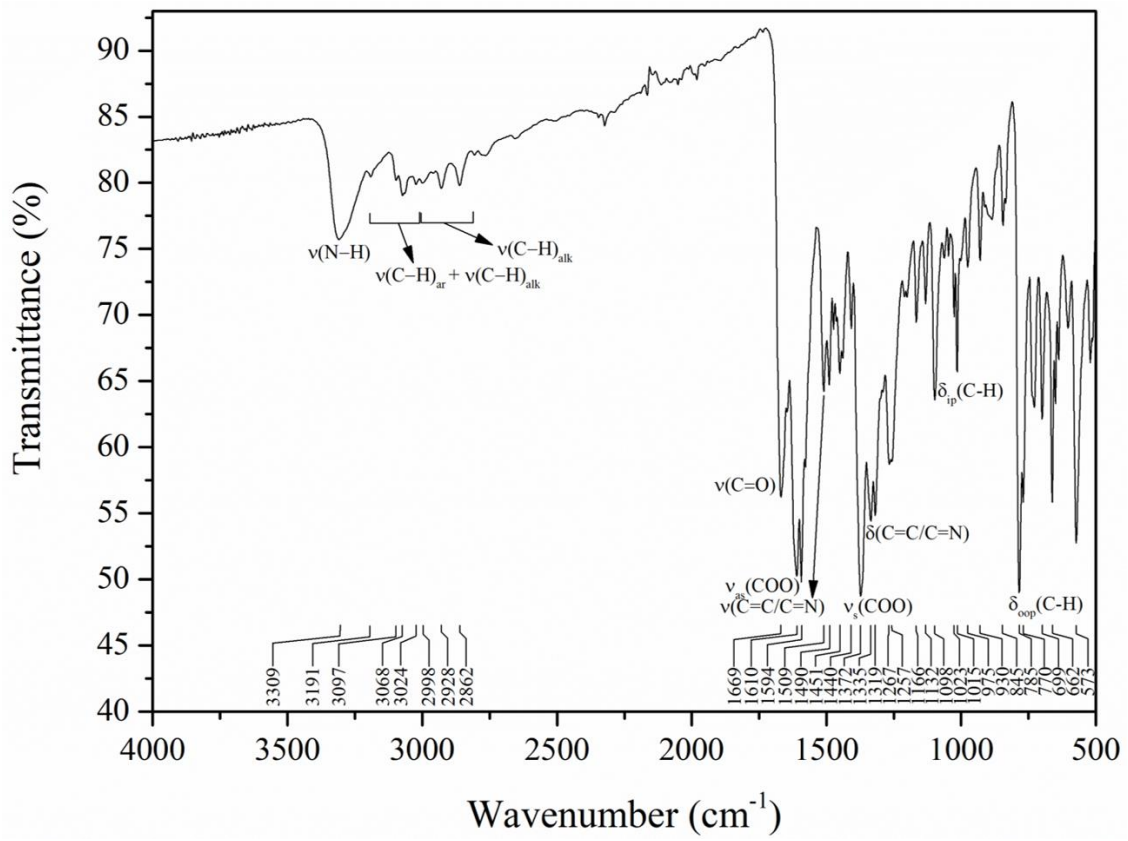

Figure S5. FTIR-ATR spectrum of compound [Zn(ACA)$_2$(terpy)]·2DMF (**5**).

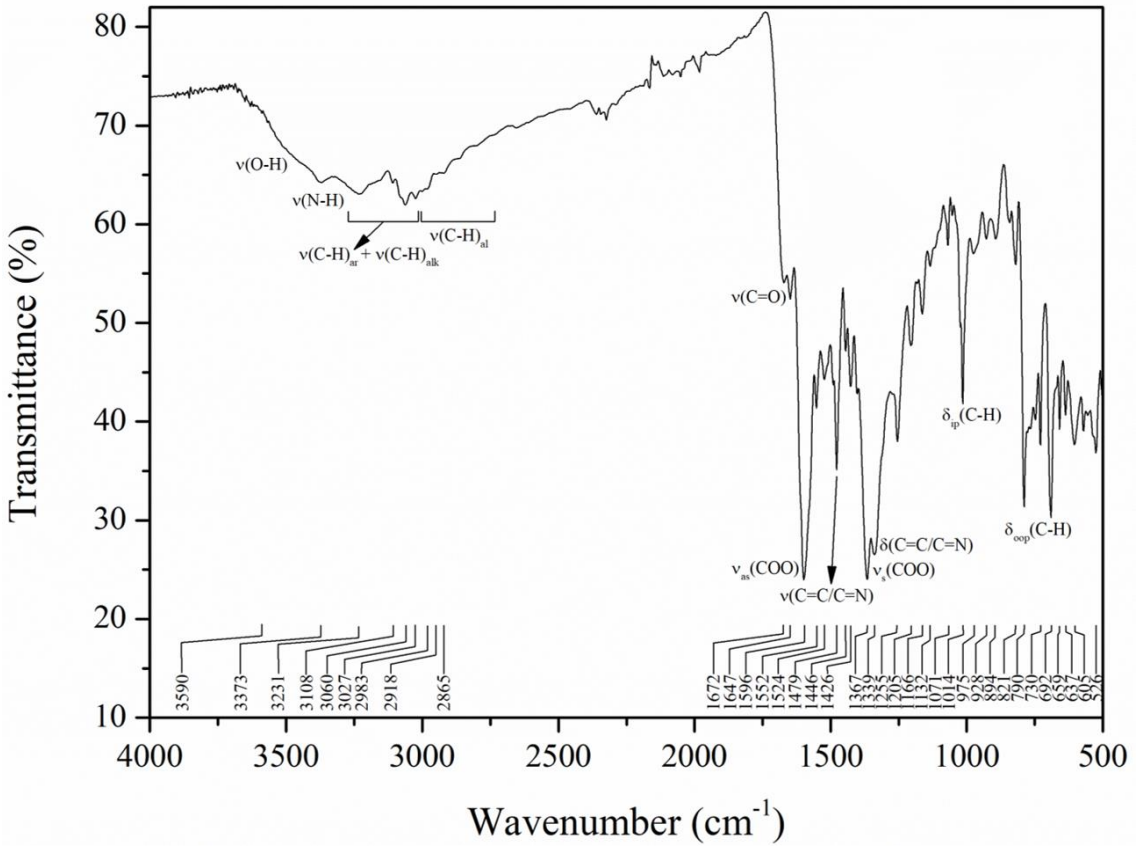

Figure S6. FTIR-ATR spectrum of compound [Zn(ACA)$_2$(mpterpy)]·4MeOH (**6**).

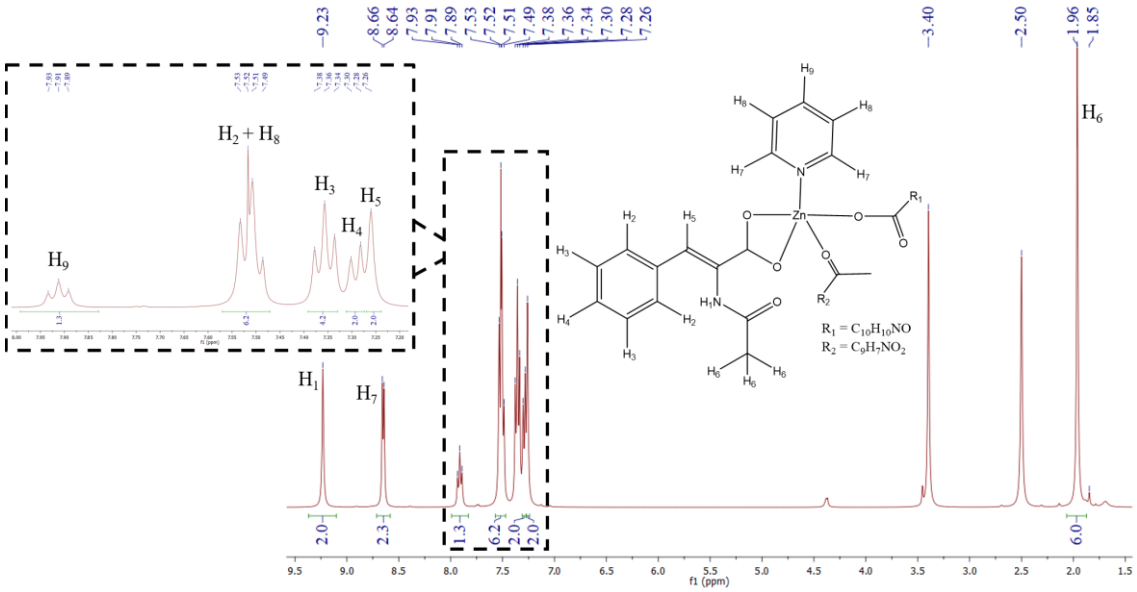

Figure S7. ^{1}H NMR spectrum of compound [Zn(μ-O,O'-ACA)(ACA)(py)]$_n$ (**1**).

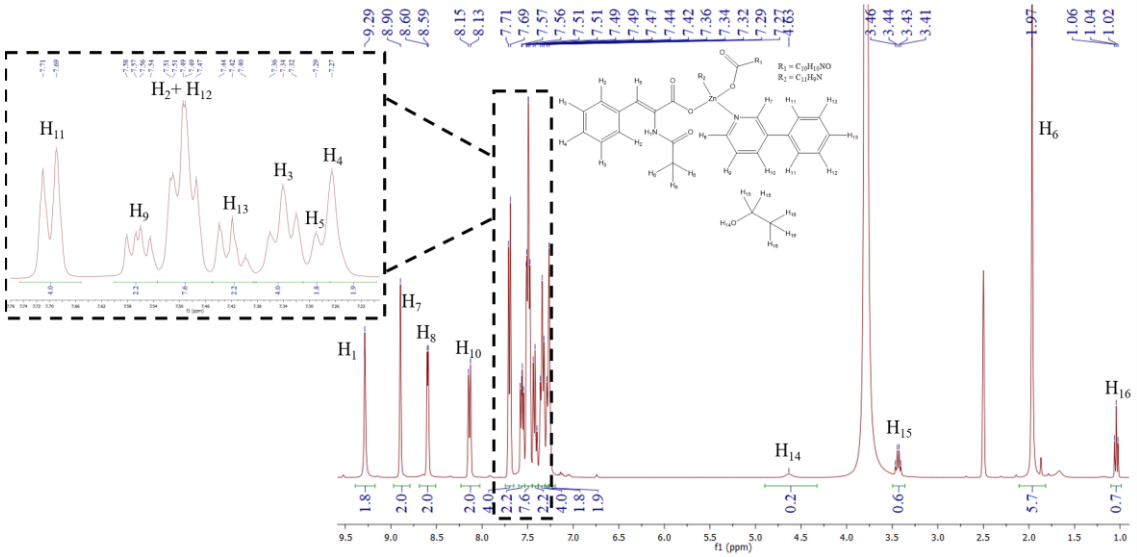

Figure S8. ^{1}H NMR spectrum of compound [Zn(ACA)$_2$(3-phpy)$_2$]·EtOH (**2**).

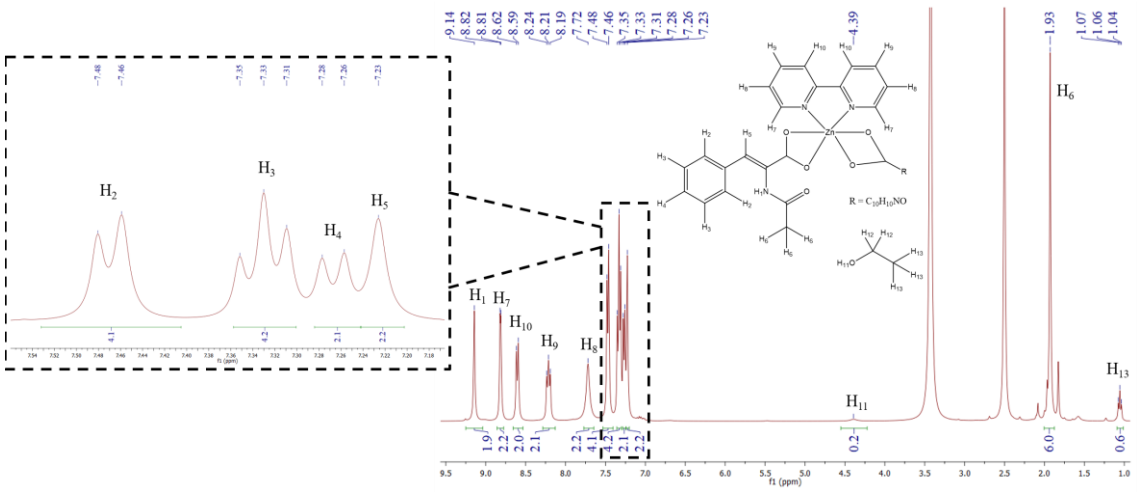

Figure S9. ^{1}H NMR spectrum of compound [Zn(ACA)$_2$(2,2'-bipy)]·4EtOH (**3**).

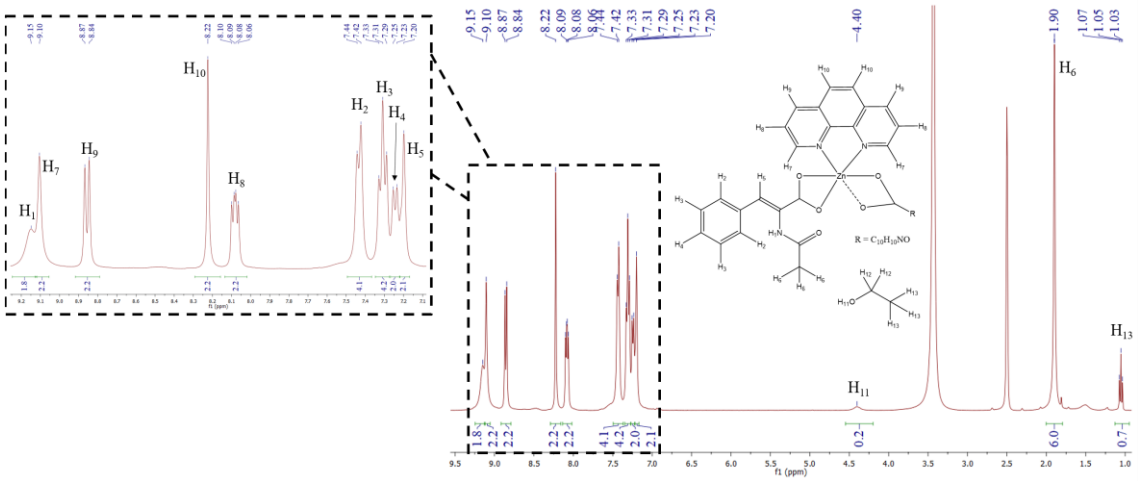

Figure S10. ^{1}H NMR spectrum of compound [Zn(ACA)$_2$(1,10-phen)][Zn(ACA)$_2$(1,10-phen)]·3EtOH (**4**).

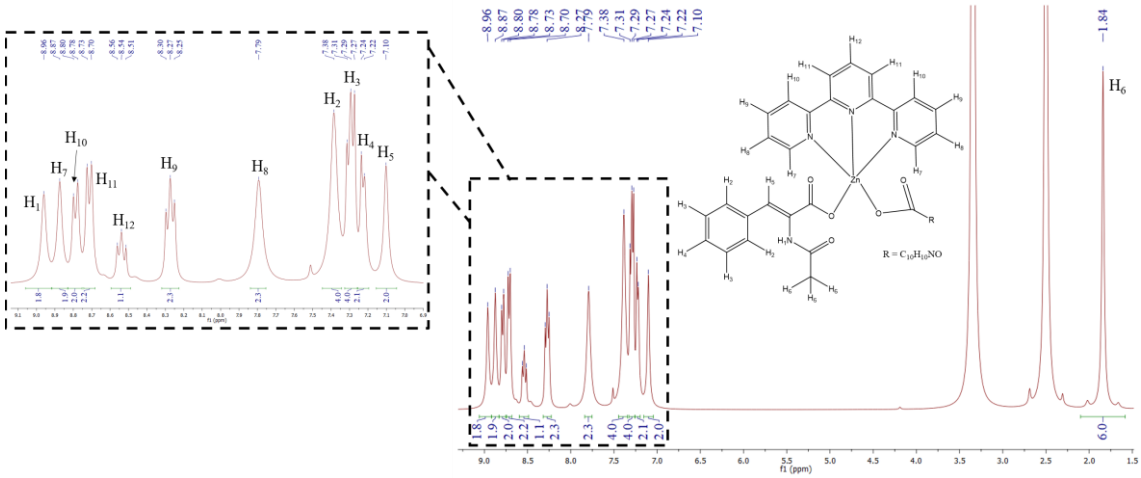

Figure S11. ^{1}H NMR spectrum of compound [Zn(ACA)$_2$(terpy)]·2DMF (**5**).

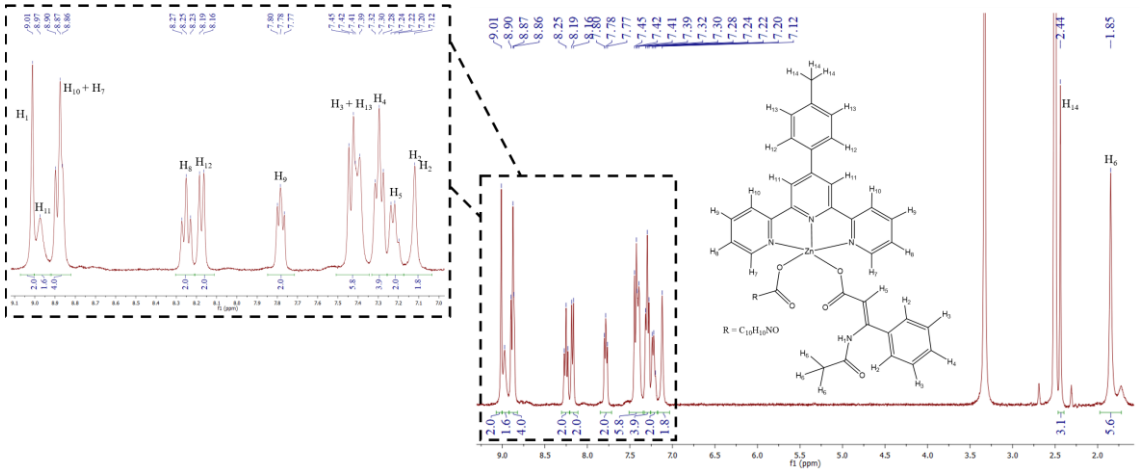

Figure S12. ^{1}H NMR spectrum of compound [Zn(ACA)$_2$(mpterpy)]·4MeOH (**6**).

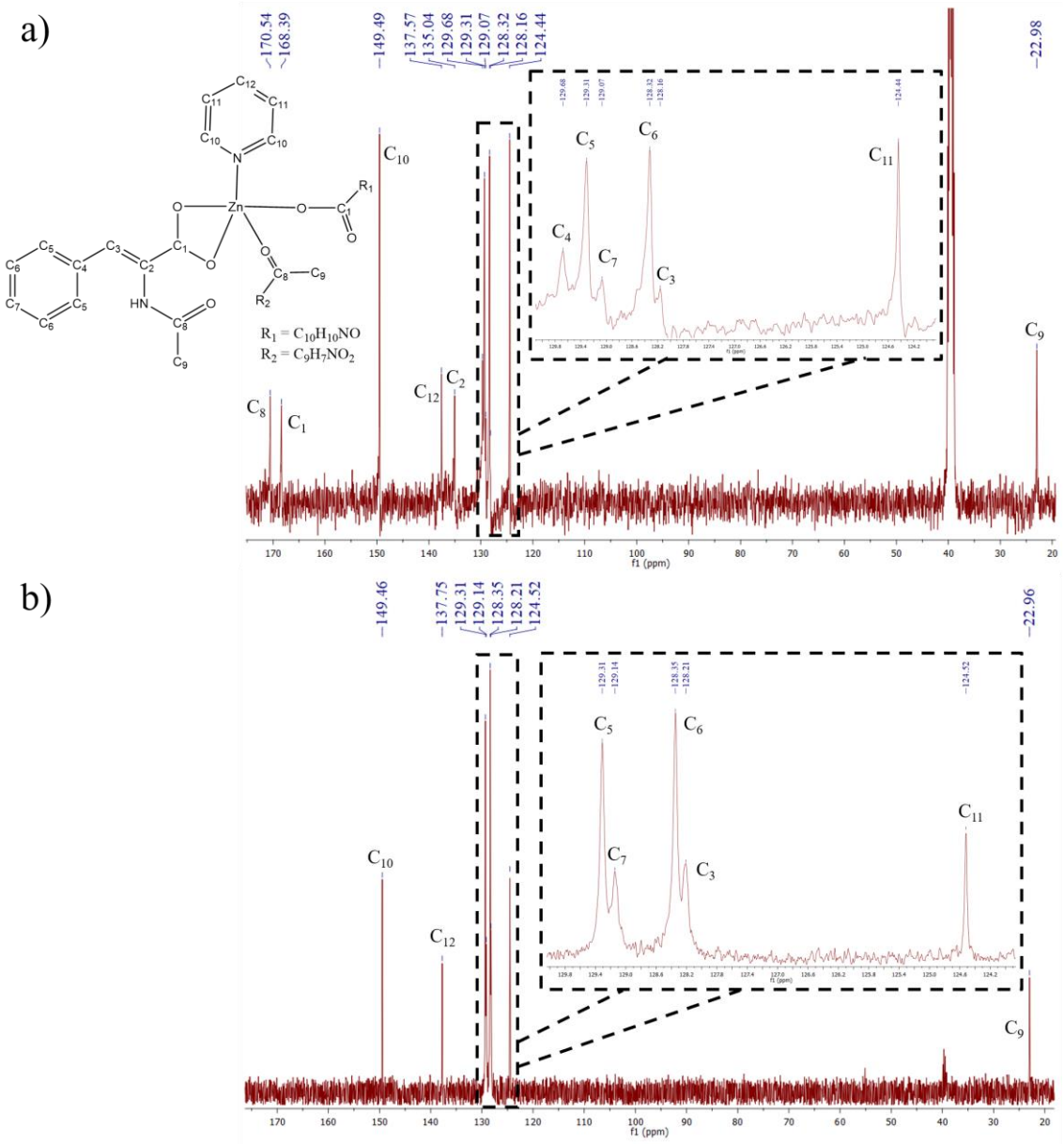

Figure S13. (a) $^{13}C\{^{1}H\}$ NMR and (b) DEPT-135 spectra of compound $[Zn(\mu\text{-}O,O'\text{-}ACA)(ACA)(py)]_n$ (**1**).

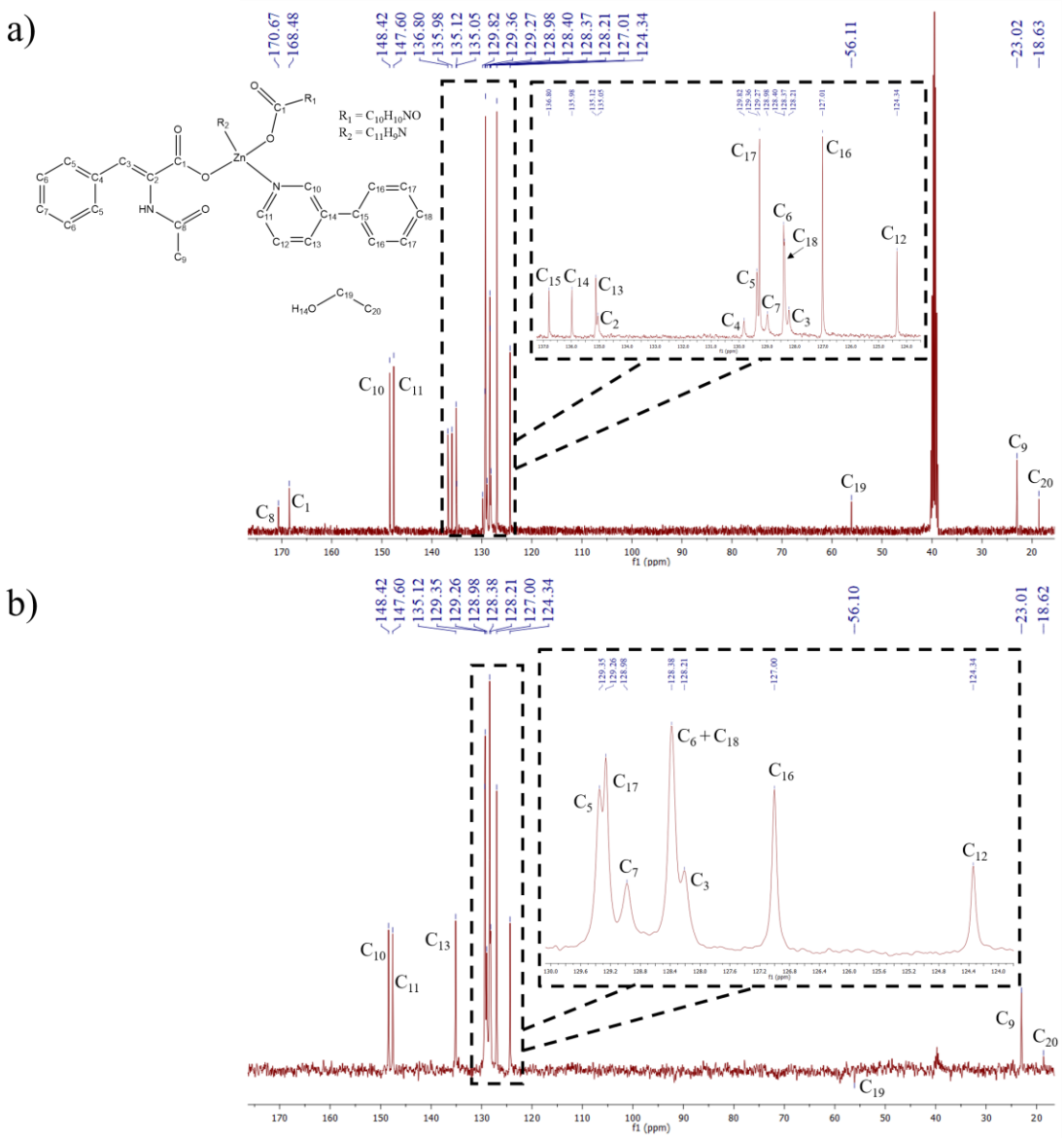

Figure S14. (a) $^{13}C\{^{1}H\}$ NMR and (b) DEPT-135 spectra of compound $[Zn(ACA)_2(3\text{-}phpy)_2]\cdot EtOH$ (**2**).

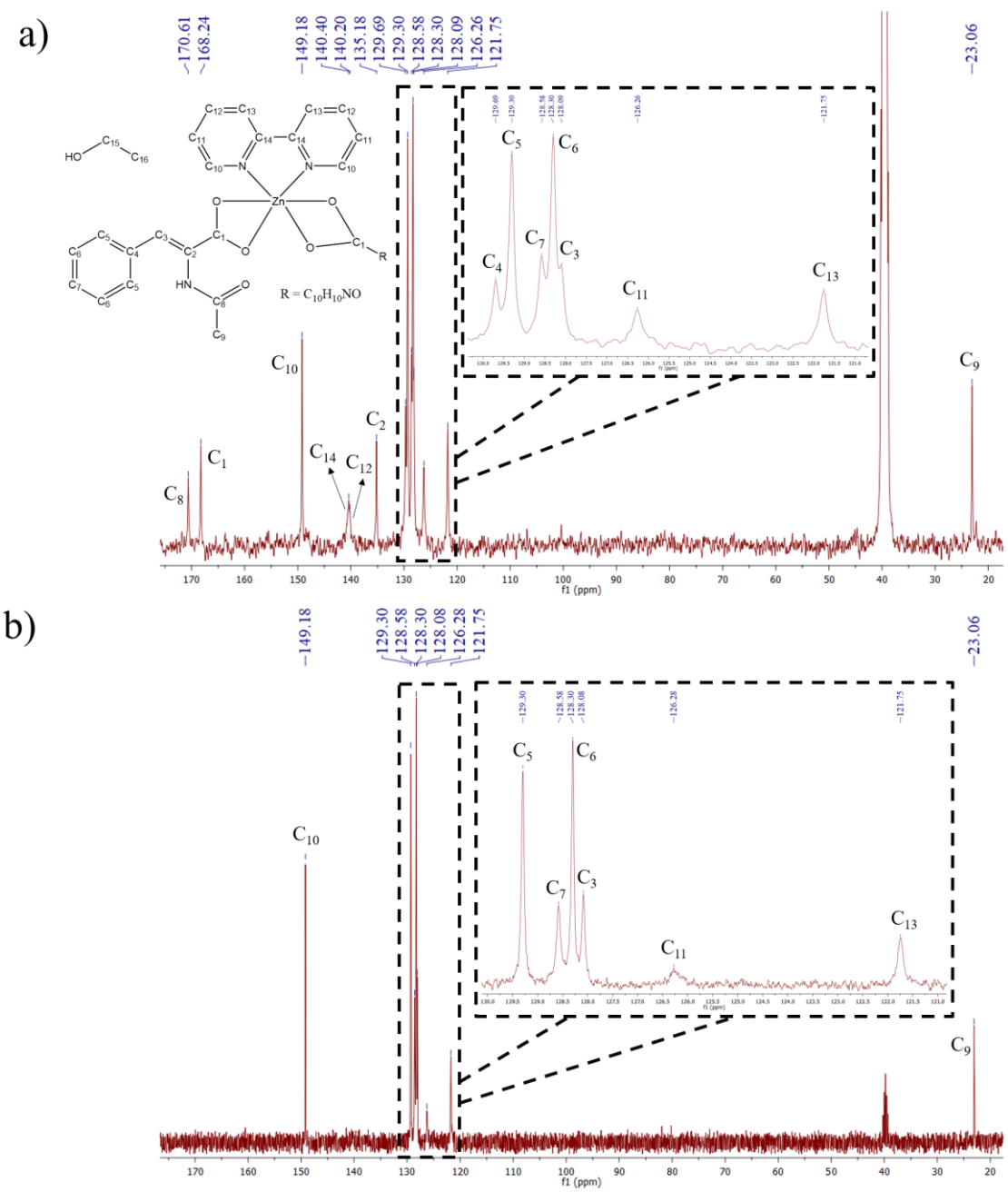

Figure S15. (a) $^{13}C\{^{1}H\}$ NMR and (b) DEPT-135 spectra of compound $[Zn(ACA)_2(2,2'\text{-bipy})]\cdot 4EtOH$ (**3**).

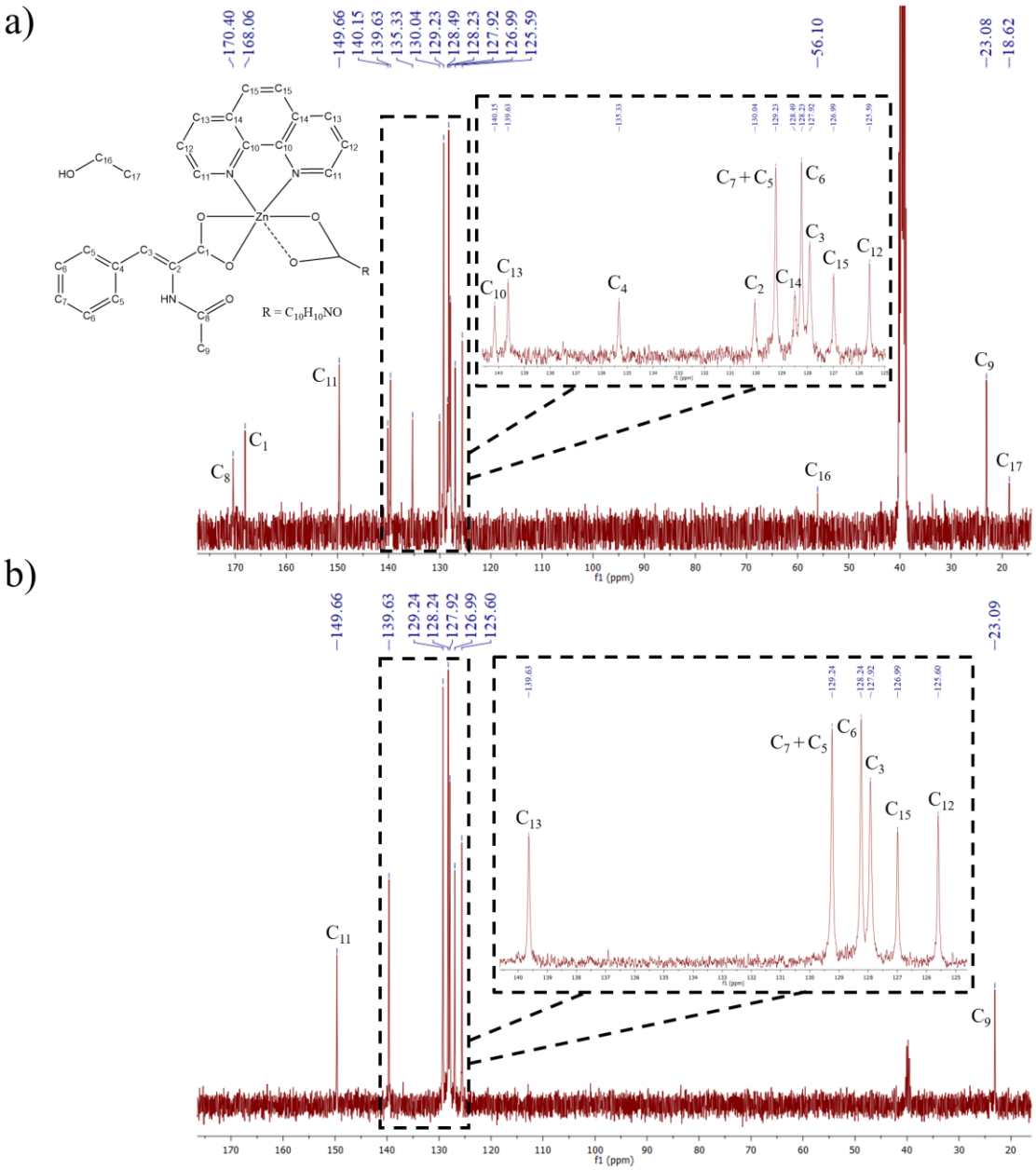

Figure S16. (a) $^{13}C\{^{1}H\}$ NMR and (b) DEPT-135 spectra of compound [Zn(ACA)$_2$(1,10-phen)][Zn(ACA)$_2$(1,10-phen)]·3EtOH (**4**).

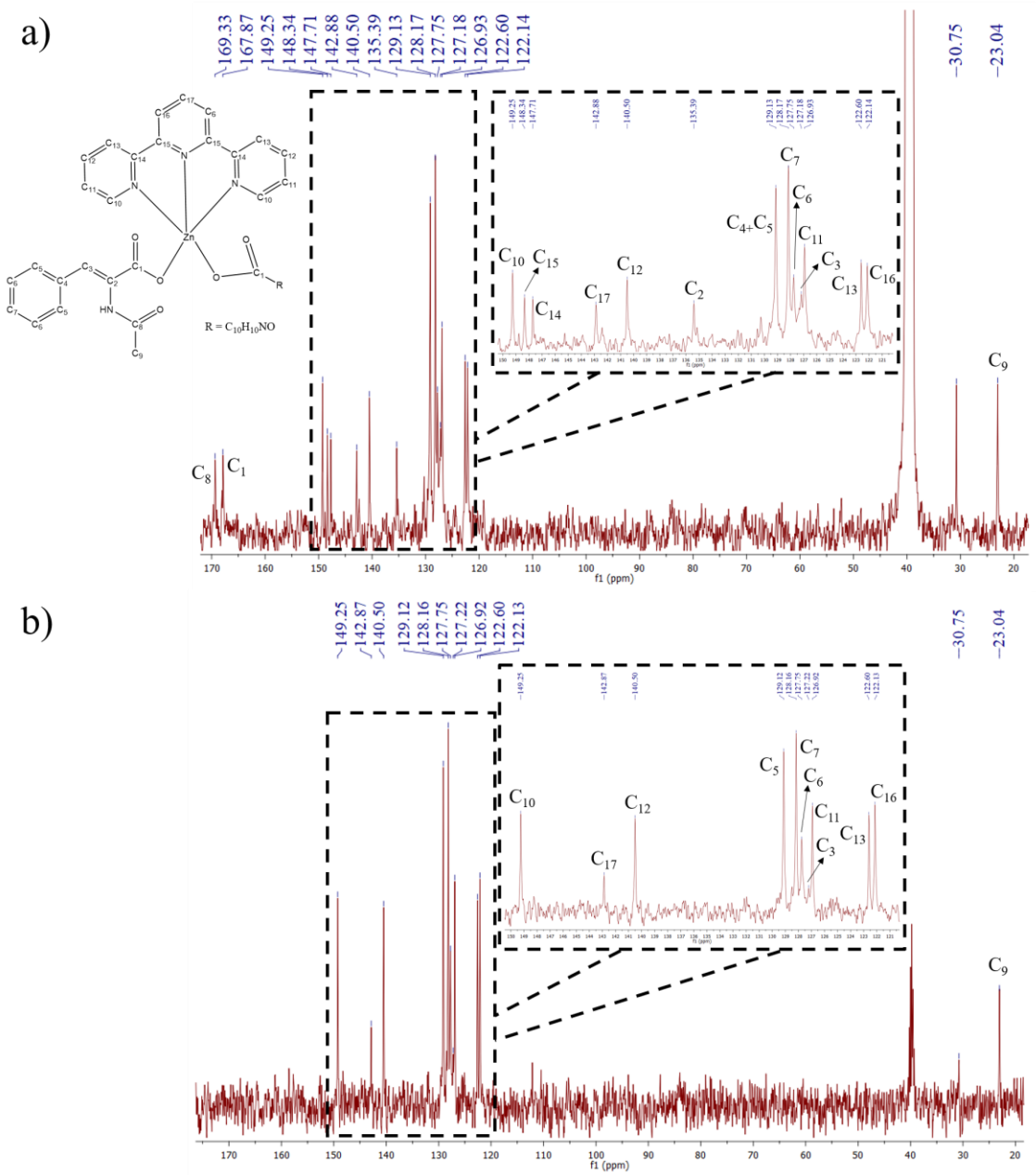

Figure S17. (a) $^{13}C\{^{1}H\}$ NMR and (b) DEPT-135 spectra of compound $[Zn(ACA)_2(terpy)]\cdot 2DMF$ (**5**).

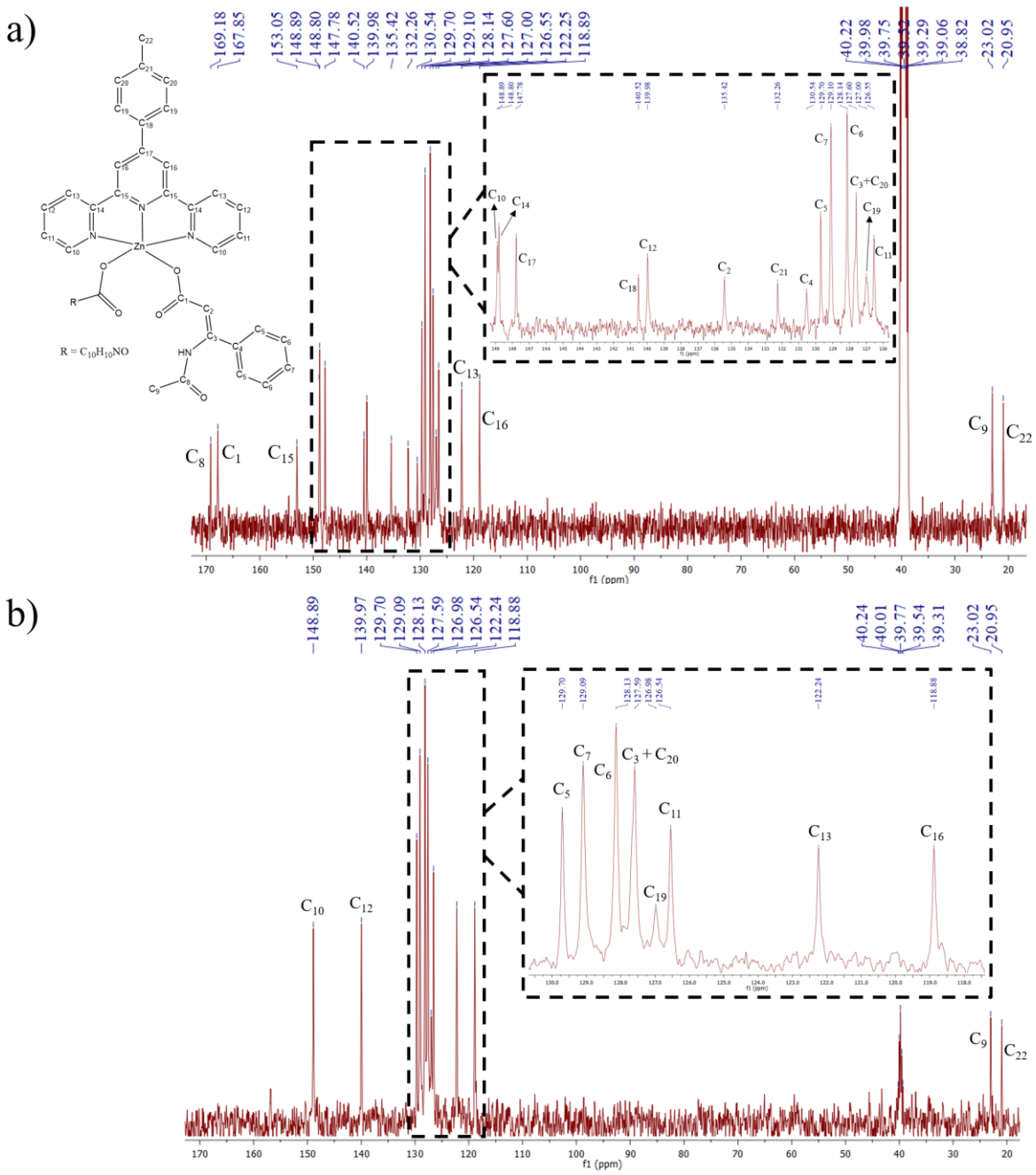

Figure S18. (a) $^{13}C\{^{1}H\}$ NMR and (b) DEPT-135 spectra of compound $[Zn(ACA)_2(mpterpy)]\cdot 4MeOH$ (**6**).

Intramolecular and Intermolecular Interactions

Table S1. Selected intra- and intermolecular interactions (Å) for **1**-**3**[a].

Complex **1**	Intramolecular interactions	D-H···A	D-H	H···A	D···A	>D-H···A	
		N(1)-H(1)···O(6)	0.88	1.98	2.843(3)	167	
		C(9)-H(9)···O(6)	0.95	2.43	3.357(3)	166	
		C(11)-H(11A)···O(6)	0.98	2.48	3.346(4)	147	
		C(23)-H(23)···O(2)	0.95	2.26	3.092(6)	147	
	Planar intramolecular interactions	Cg(I)···Cg(J)	d_{Cg-Cg}[b]	α[c]	β, γ[d]	$d_{plane-plane}$[e]	d_{offset}[f]
		Cg(1)···Cg(2)	3.714(2)	17.4(2)	34.8, 19.4	3.502(2), 3.050 (1)	1.237, 2.120
	Intermolecular interactions	D-H···A	D-H	H···A	D···A	>D-H···A	
		N(2)-H(2)···O(4)	0.88	1.99	2.836(3)	162	
		C(18)-H(18)···O(2)	0.95	2.46	3.407(3)	173	
Complex **2**	Intermolecular interactions	D-H···A	D-H	H···A	D···A	>D-H···A	
		N(1)-H(1)···O(2)	0.88	2.05	2.857(3)	153	
		C(23)-H(23)···O(1)	0.95	2.35	3.267(3)	162	
		C(31)-H(31)···Cg(1)	0.95	2.90	3.686(4)	140	
		C(8)-H(8)···Cg(1)	0.95	2.89	3.606(4)	133	
Complex **3**	Intermolecular interactions	D-H···A	D-H	H···A	D···A	>D-H···A	
		C(25)-H(25)···O(6)	0.95	2.38	3.184(6)	142	
		C(29)-H(29)···O(5)	0.95	2.39	3.254(4)	151	
		N(1)-H(1N)···O(2)	0.88	1.99	2.839(4)	162	
		C(11)-H(11A)···O(4)	0.98	2.59	3.518(5)	157	
		O(1W)-H(1W)···O(3)	0.82(3)	2.15(3)	2.957(4)	172(3)	
		O(2W)-H(2W)···O(1W)	0.84	1.86	2.687(5)	166	
		O(3W)-H(3W)···O(2W)	0.84	1.87	2.702(5)	171	
		O(4W)-H(4W)···O(3W)	0.84	1.90	2.708(4)	162	
		N(2)-H(2N)···O(3W)	0.84	2.01	2.809(4)	159	
		C(20)-H(20)···O(1)	0.95	2.57	3.336(4)	138	
	Planar intermolecular interactions	Cg(I)···Cg(J)	d_{Cg-Cg}[b]	α[c]	β, γ[d]	$d_{plane-plane}$[e]	d_{offset}[f]
		Cg(3)···Cg(4)	3.763(2)	7.6(2)	25.8, 19.1	3.556(2), 3.387(2)	1.230, 1.640

[a] All the distances are given in (Å) and the angles in (º). [b] Centroid-centroid distance. [c] Dihedral angle between the ring planes. [d] Offset angles: angle between Cg(I)-Cg(J) vector and normal to plane I, angle between Cg(I)-Cg(J) vector and normal to plane J (β = γ, when α = 0). [e] Perpendicular distance of Cg(I) on plane J and perpendicular distance of Cg(J) on plane I (equal when α = 0). [f] Horizontal displacement or slippage between Cg(I) and Cg(J) (equal for both centroids when α = 0). **1**: Cg(1) = C(4) C(5) C(6) C(7) C(8) C(9); Cg(2) = N(3) C(23) C(24) C(25) C(26) C(27). **2**: Cg(1) = C(4) C(5) C(6) C(7) C(8) C(9). **3**: Cg(3) = N(3) C(23) C(24) C(25) C(26) C(27); Cg(4) = N(4) C(28) C(29) C(30) C(31) C(32).

Table S2. Selected intermolecular interactions (Å) for **4**-**6**[a].

Complex **4**	Intermolecular interactions	D-H···A	D-H	H···A	D···A	>D-H···A	
		N(1A)-H(1NA)···O(2B)	0.88	1.95	2.784(6)	156	
		N(1B)-H(1NB)···O(1A)	0.88	2.02	2.848(6)	157	
		C(25A)-H(25A)···O(6B)	0.95	2.37	3.291(9)	164	
		C(27A)-H(27A)···O(4B)	0.95	2.57	3.276(8)	131	
		C(25B)-H(25B)···O(6A)	0.95	2.28	3.175(9)	158	
		N(2B)-H(2NB)···O(2W)	0.88	2.23	3.049(7)	155	
		O(2W)-H(2WO)···O(3B)	0.84	2.10	2.910(6)	161	
		N(2A)-H(2NA)···O(1W)	0.88	1.97	2.812(7)	160	
		O(1W)-H(1WO)···O(3W)	0.84	1.86	2.704(7)	176	
		C(24A)-H(24A)···O(1W)	0.95	2.40	3.122(9)	132	
		C(5W)-H(5WB)···Cg(5)	0.99	2.84	3.816(7)	159	
		O(3W)-H(3WO)···O(3A)	0.84	1.92	2.742(6)	168	
		C(7A)-H(7A)···O(3B)	0.95	2.61	3.546(7)	170	
		C(7B)-H(7B)···O(3A)	0.95	2.50	3.446(7)	171	
	Planar intermolecular interactions	Cg(I)···Cg(J)	d_{Cg-Cg}[b]	α[c]	β, γ[d]	$d_{plane-plane}$[e]	d_{offset}[f]
		Cg(3)···Cg(4)	3.515(4)	0.6(3)	13.2, 13.8	3.413(3), 3.423(3)	0.841, 0.799
		Cg(6)···Cg(6)	3.664(4)	3.2(3)	20.7, 22.1	3.394(3), 3.428(3)	1.380, 1.293
		Cg(3)···Cg(7)	3.645(4)	4.3(3)	23.0, 26.9	3.250(3), 3.356(3)	1.650, 1.422
Complex **5**	Intermolecular interactions	D-H···A	D-H	H···A	D···A	>D-H···A	
		C(19)-H(19A)···O(1)	0.93	2.44	3.221(4)	142	
		N(1)-H(1A)···O(4)	0.86	1.95	2.78(2)	162	
		C(14)-H(14)···O(2)	0.93	2.49	3.225(6)	136	
		C(15A)-H(15)···O(3)	0.93	2.51	3.406(5)	163	
Complex **6**	Intermolecular interactions	D-H···A	D-H	H···A	D···A	>D-H···A	
		N(1)-H(1)···O(2)	0.88	2.00	2.858(3)	164	
		C(26)-H(26)···O(3)	0.95	2.38	3.264(3)	155	
		C(29)-H(29)···O(3)	0.95	2.40	3.237(4)	147	
		C(43)-H(43)···O(3)	0.95	2.42	3.370(4)	177	
		N(2)-H(2N)···O(1W)	0.88	2.28	3.074(4)	150	
		O(1W)-H(1W)···O(1)	0.98(5)	1.82(5)	2.794(3)	173(4)	
		O(2W)-H(2WO)···O(1W)	0.84	2.46	3.235(5)	153	
		C(36)-H(36)···O(3W)	0.95	2.31	3.162(5)	149	
		O(3W)-H(3WO)···O(4WO)	0.84	1.88	2.717(6)	172	
		O(4W)-H(4WO)···O(5)	0.84	1.96	2.783(4)	166	
		C(31)-H(31)···O(5)	0.95	2.56	3.484(4)	166	
		C(34)-H(34)···O(5)	0.95	2.28	3.221(3)	169	
	Planar intermolecular interactions	Cg(I)···Cg(J)	d_{Cg-Cg}[b]	α[c]	β, γ[d]	$d_{plane-plane}$[e]	d_{offset}[f]
		Cg(1)···Cg(2)	3.613(2)	3.7(2)	17.4, 21.1	3.372(1), 3.448(1)	1.299, 1.082

[a] All the distances are given in (Å) and the angles in (º). [b] Centroid-centroid distance. [c] Dihedral angle between the ring planes. [d] Offset angles: angle between Cg(I)-Cg(J) vector and normal to plane I, angle between Cg(I)-Cg(J) vector and normal to plane J (β = γ, when α = 0). [e] Perpendicular distance of Cg(I) on plane J and perpendicular distance of Cg(J) on plane I (equal when α = 0). [f] Horizontal displacement or slippage between Cg(I) and Cg(J) (equal for both centroids when α = 0). **4**: Cg(3) = C(26A) C(27A) C(28A) C(29A) C(33A) C(34A); Cg(4) = C(26B) C(27B) C(28B) C(29B) C(33B) C(34B); Cg(5) = C(15A) C(16A) C(17A) C(18A) C(19A) C(20A); Cg(6) = C(4A) C(5A) C(6A) C(7A) C(8A) C(9A); Cg(7) = C(4B) C(5B) C(6B) C(7B) C(8B) C(9B). **6**: Cg(1) = N(4) C(28) C(29)C(30) C(31) C(32); Cg(2) = N(5) C(33) C(34) C(35) C(36) C(37)

UV-Vis and Fluorescence Spectroscopies

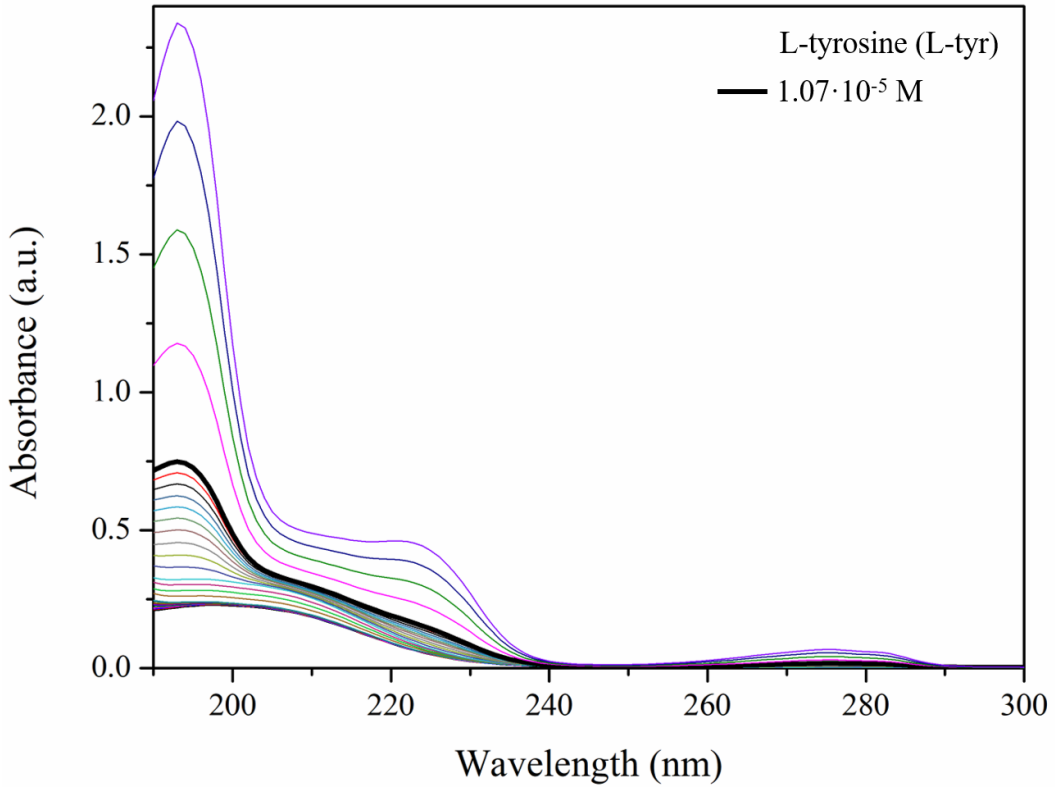

Figure S19. UV-Vis spectrum of L-tyrosine reference (L-tyr) in Milli-Q water solutions at RT. Bold black line indicates the concentration from which the aggregation begins.

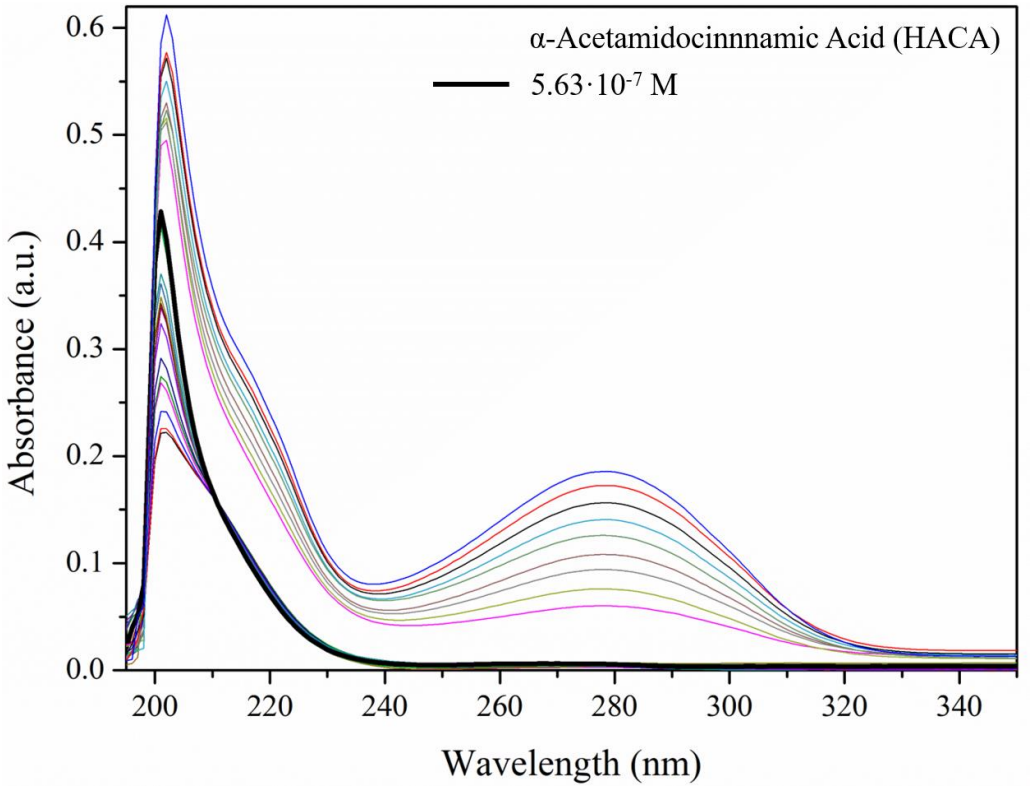

Figure S20. UV-Vis spectrum of α-acetamidocinnamic acid (HACA) in EtOH solutions at RT. Bold black line indicates the concentration from which the aggregation begins.

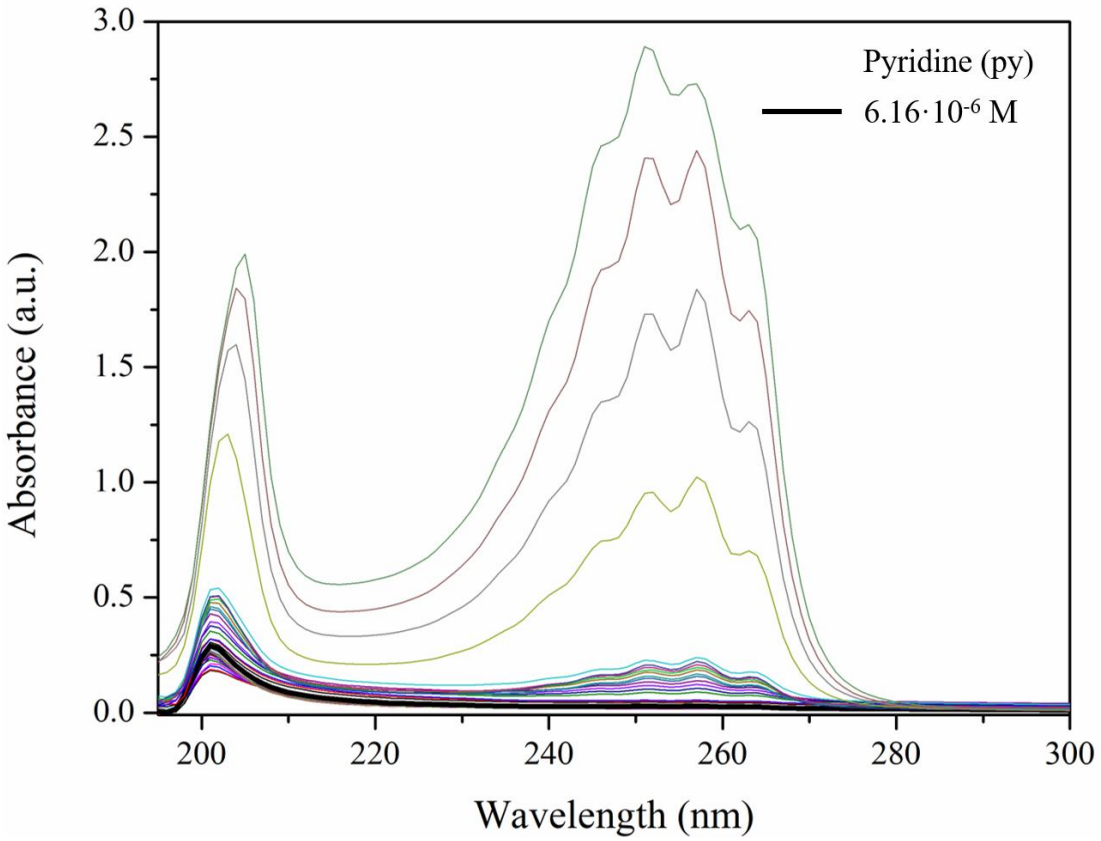

Figure S21. UV-Vis spectrum of pyridine (py) in EtOH solutions at RT. Bold black line indicates the concentration from which the aggregation begins.

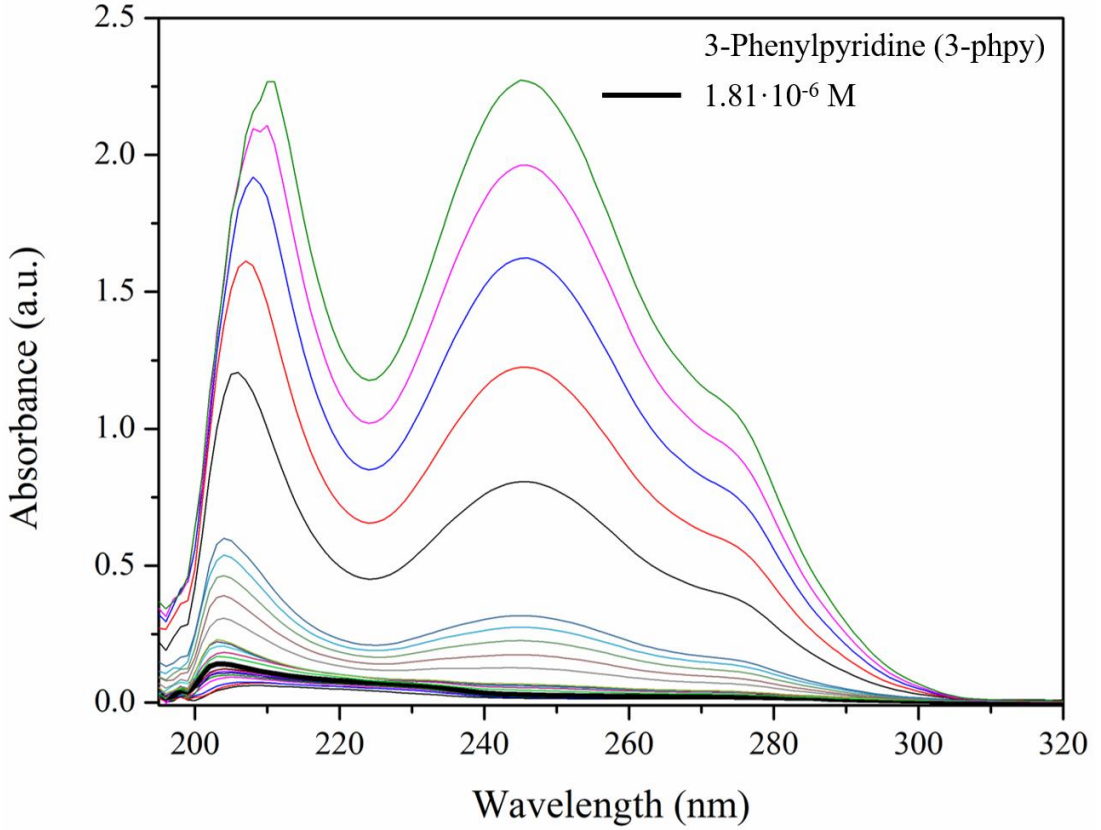

Figure S22. UV-Vis spectrum of 3-phenylpyridine (3-phpy) in MeOH solutions at RT. Bold black line indicates the concentration from which the aggregation begins.

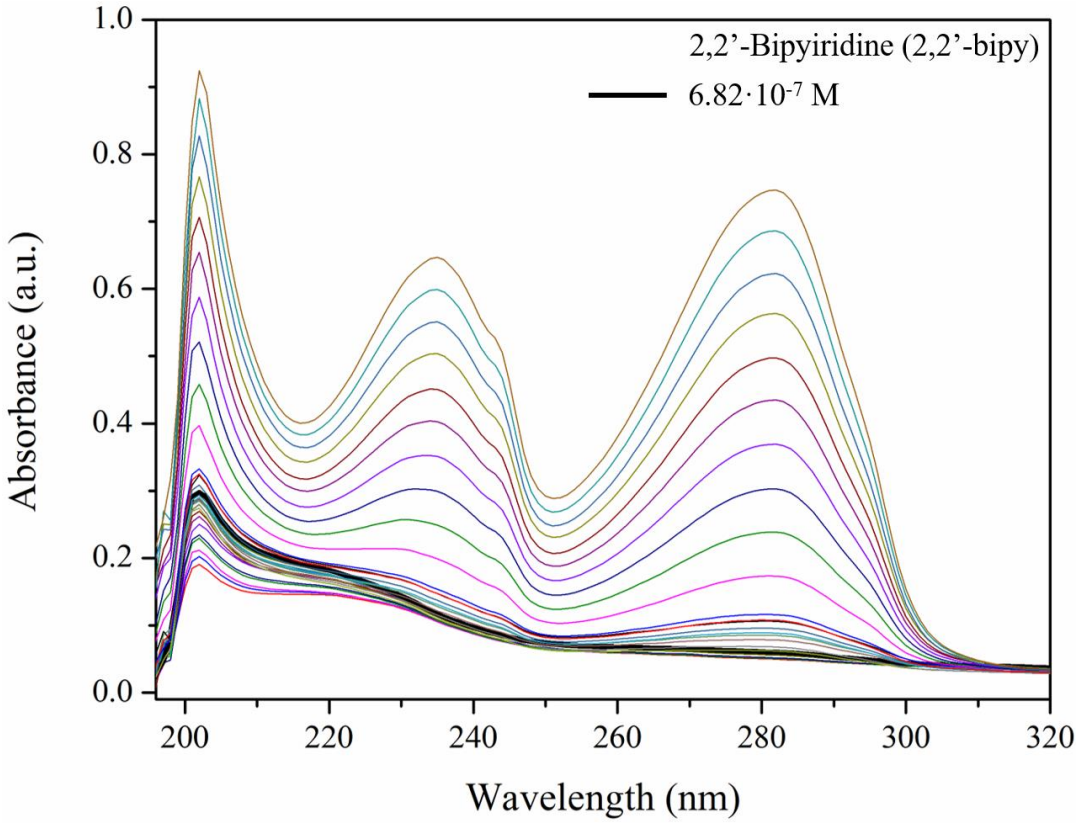

Figure S23. UV-Vis spectrum of 2,2'-bipyridine (2,2'-bipy) in MeOH solutions at RT. Bold black line indicates the concentration from which the aggregation begins.

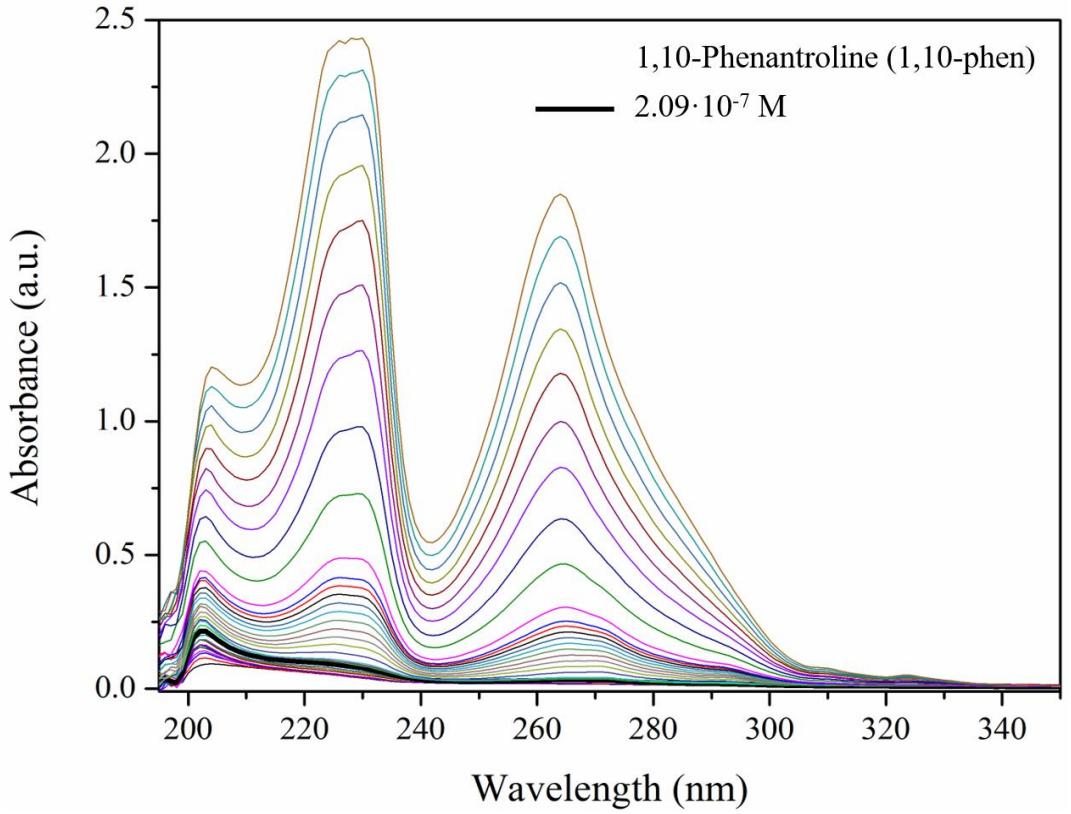

Figure S24. UV-Vis spectrum of 1,10-phenantroline (1,10-phen) in MeOH solutions at RT. Bold black line indicates the concentration from which the aggregation begins.

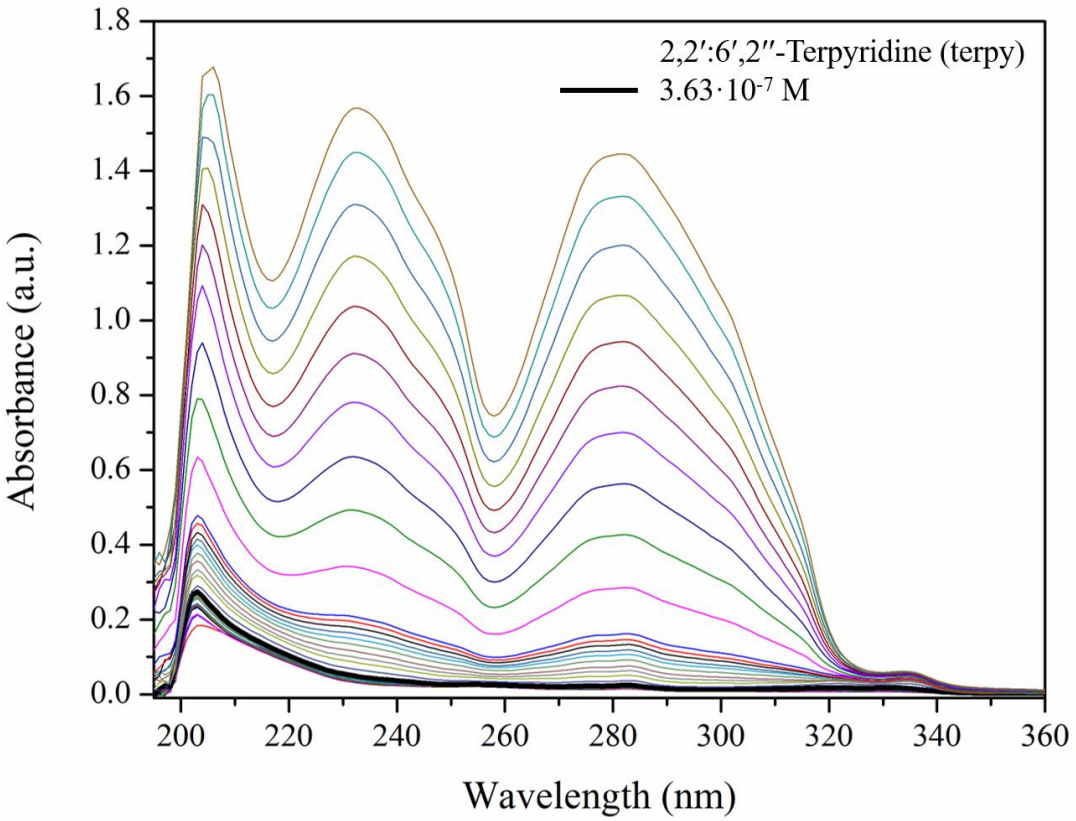

Figure S25. UV-Vis spectrum of 2,2′:6′,2″-terpyridine (terpy) in MeOH solutions at RT. Bold black line indicates the concentration from which the aggregation begins.

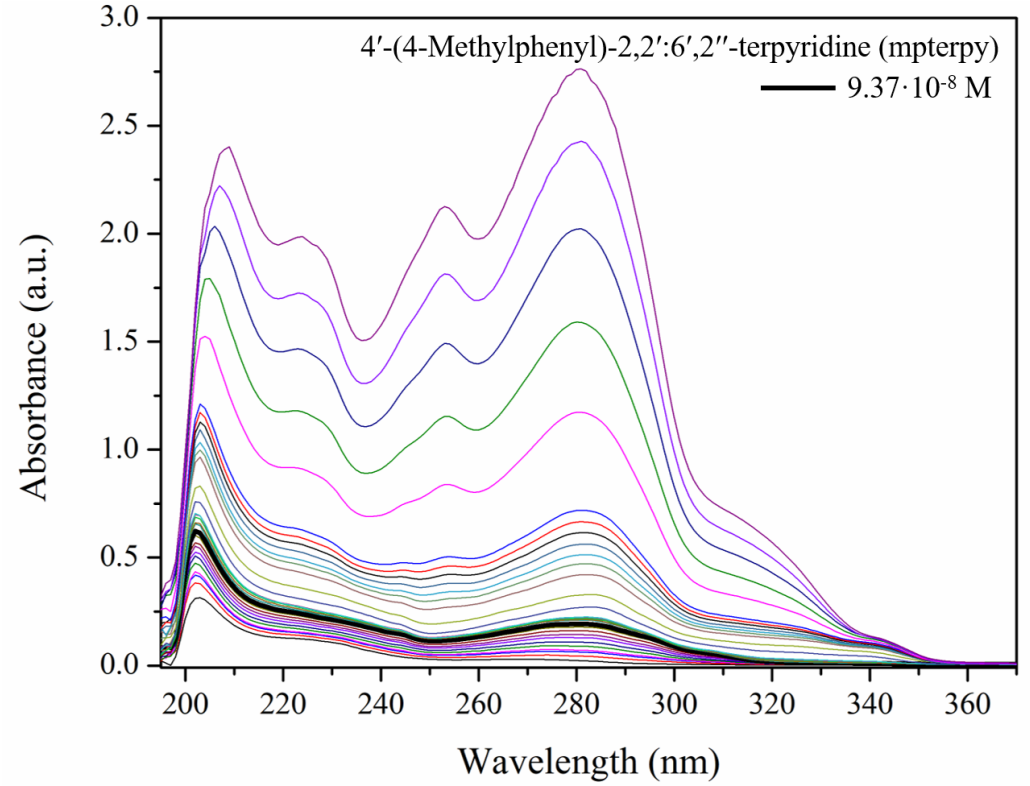

Figure S26. UV-Vis spectrum of 4’-(4-Methylphenyl)-2,2′:6′,2″-terpyridine (mpterpy) in EtOH solutions at RT. Bold black line indicates the concentration from which the aggregation begins.

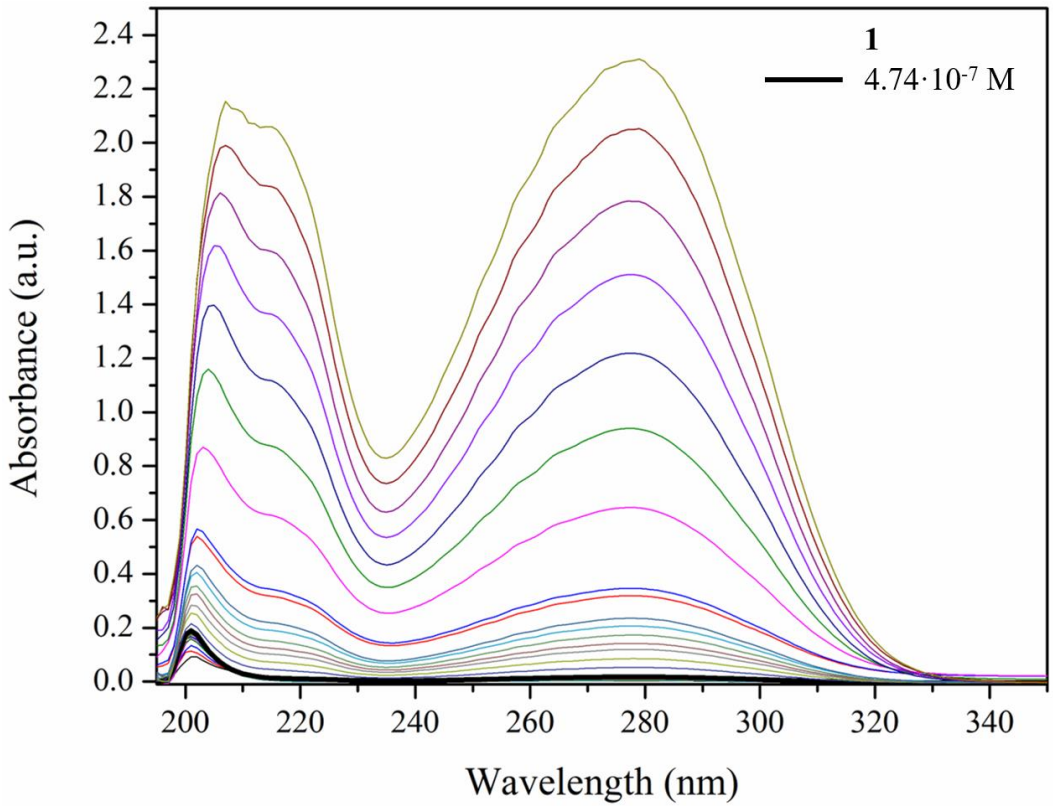

Figure S27. UV-Vis spectrum of **1** in EtOH solutions at RT. Bold black line indicates the concentration from which the aggregation begins.

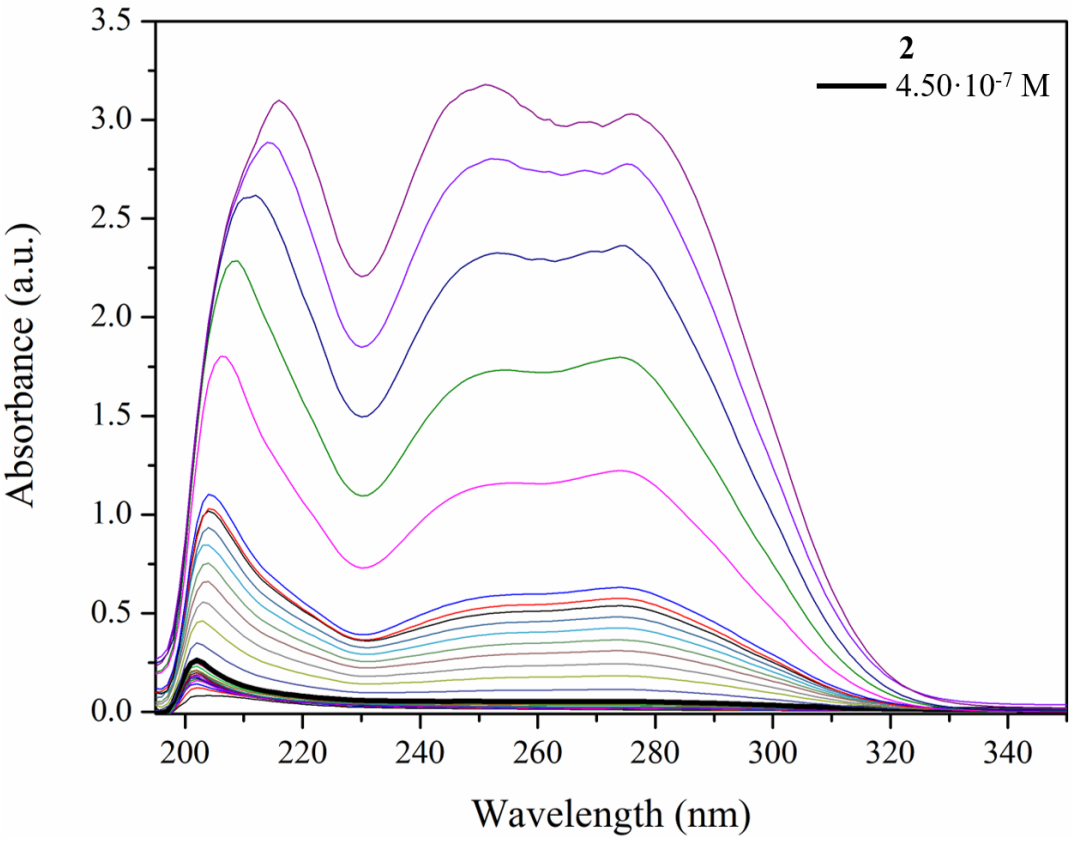

Figure S28. UV-Vis spectrum of **2** in EtOH solutions at RT. Bold black line indicates the concentration from which the aggregation begins.

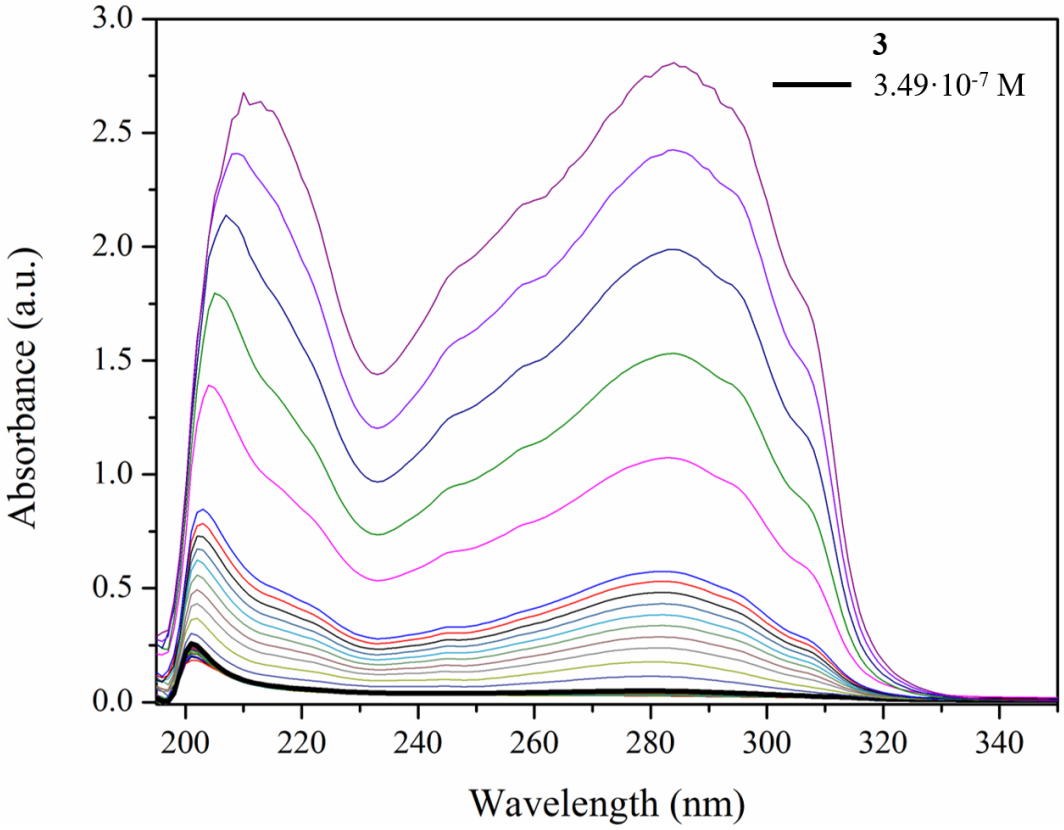

Figure S29. UV-Vis spectrum of **3** in EtOH solutions at RT. Bold black line indicates the concentration from which the aggregation begins.

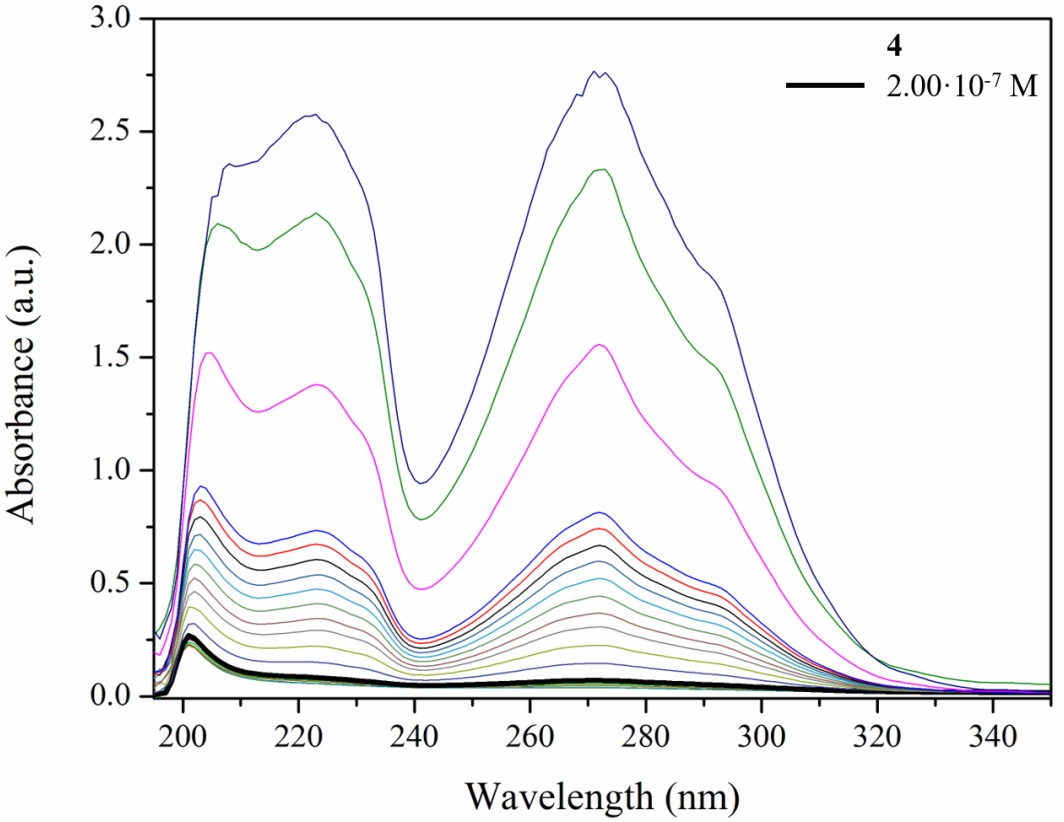

Figure S30. UV-Vis spectrum of **4** in EtOH solutions at RT. Bold black line indicates the concentration from which the aggregation begins.

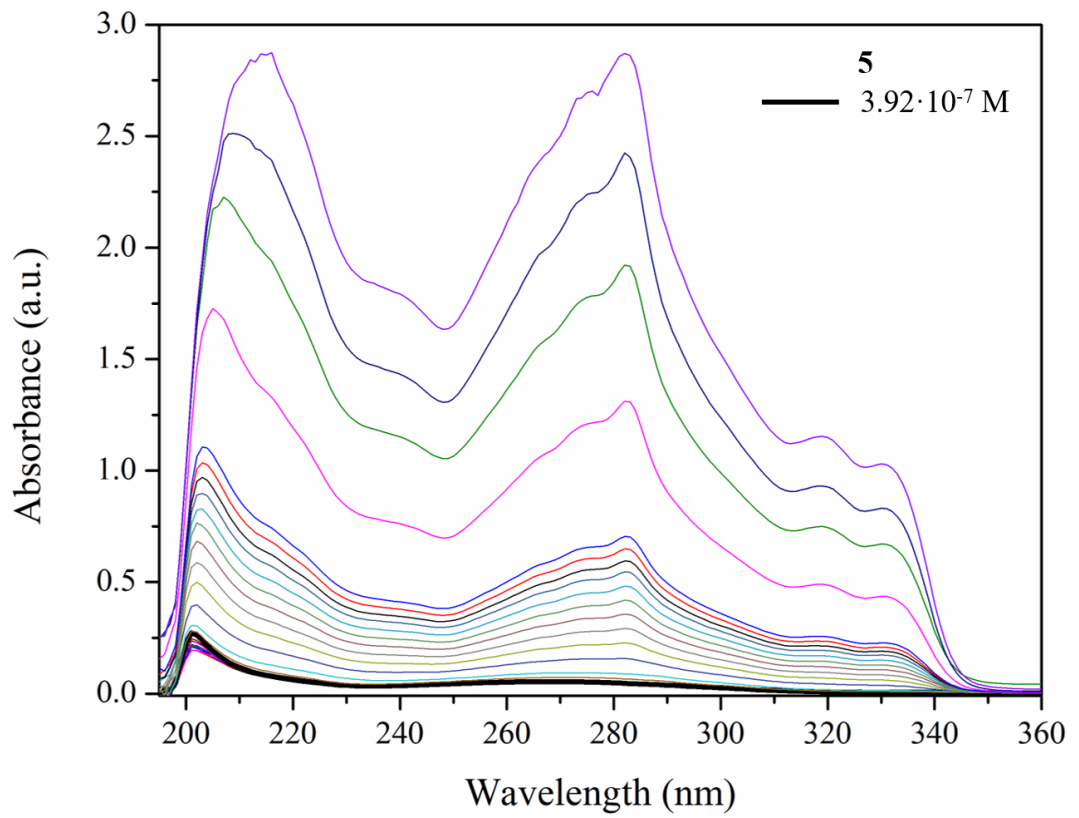

Figure S31. UV-Vis spectrum of **5** in EtOH solutions at RT. Bold black line indicates the concentration from which the aggregation begins.

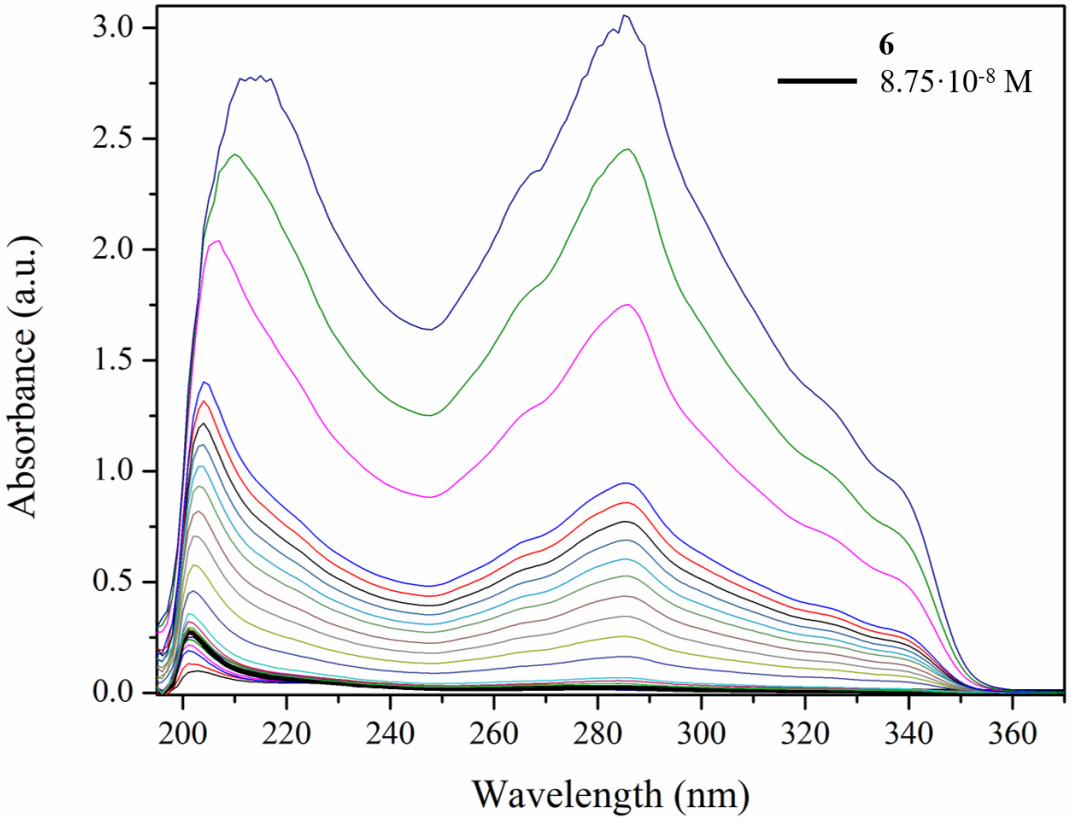

Figure S32. UV-Vis spectrum of **6** in EtOH solutions at RT. Bold black line indicates the concentration from which the aggregation begins.

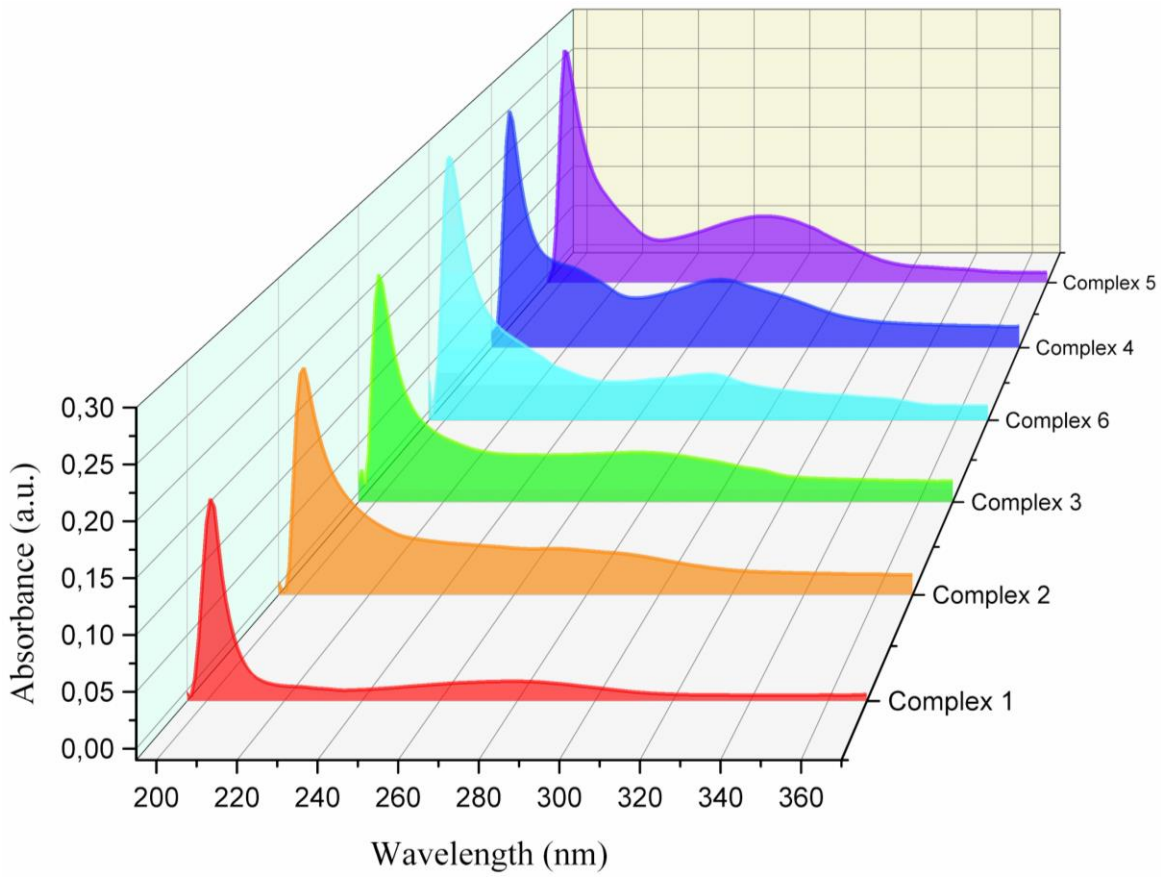

Figure S33. UV-Vis spectra of complexes **1**-**6** recorded at 298 K at concentration of ~$2 \cdot 10^{-7}$ M.

Table S3. Detailed parameters extracted from the photophysical properties of L-tyr, HACA and dPy ligands[a].

Sample	$\lambda_{max\text{-}Abs}$ (log(ε))	λ_{ex} (nm)	$\lambda_{max\text{-}em}$ (nm)
L-tyr	193 (4.65), 276 (3.11)	231 232 234 294	313 314 314 344
HACA	202 (6.05), 278 (4.14)	231 232 234 294	343 342 343 349
py	201 (5.92), 245 (3.18), 251 (3.27), 257 (3.29), 263 (3.14)	234	331
3-phpy	203 (4.90), 244 (3.97)	231	332
2,2'-bipy	202 (6.31), 280 (3.95)	232	344
1,10-phen	203 (5.81), 267 (4.25), 324 (2.63)	232	347
terpy	203 (5.66), 232 (4.28), 275 (4.23), 283 (4.25)	232	351
mpterpy	203 (6.48), 274 (6.23), 342 (4.79)	294	376

[a]All the wavelengths are given in nm. ε values are given in $M^{-1} \cdot cm^{-1}$. $\lambda_{max\text{-}Abs}$ = maximum of absorption. λ_{ex} = excitation wavelength; $\lambda_{max\text{-}em}$ = maximum of emission

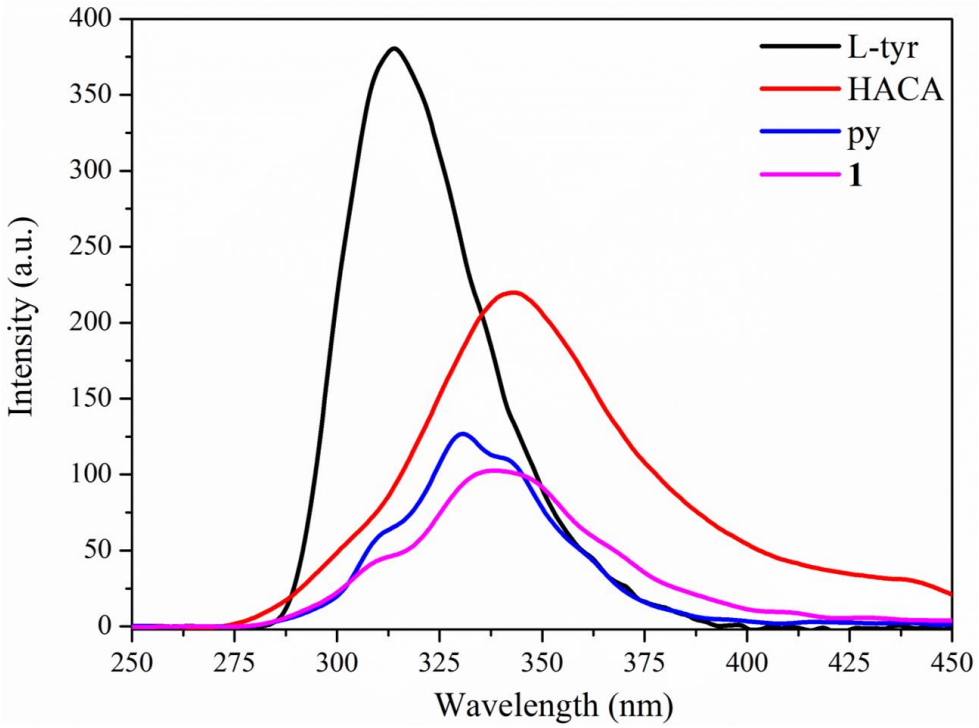

Figure S34. Emission spectra of compound **1**, HACA py and L-tyrosine, excited at 234 nm at 298K in Milli-Q water solution ($2.21 \cdot 10^{-6}$ M for L-tyrosine) or EtOH solutions ($2.50 \cdot 10^{-7}$ M for HACA, $6.01 \cdot 10^{-6}$ M for py and $3.54 \cdot 10^{-7}$ M for **1**).

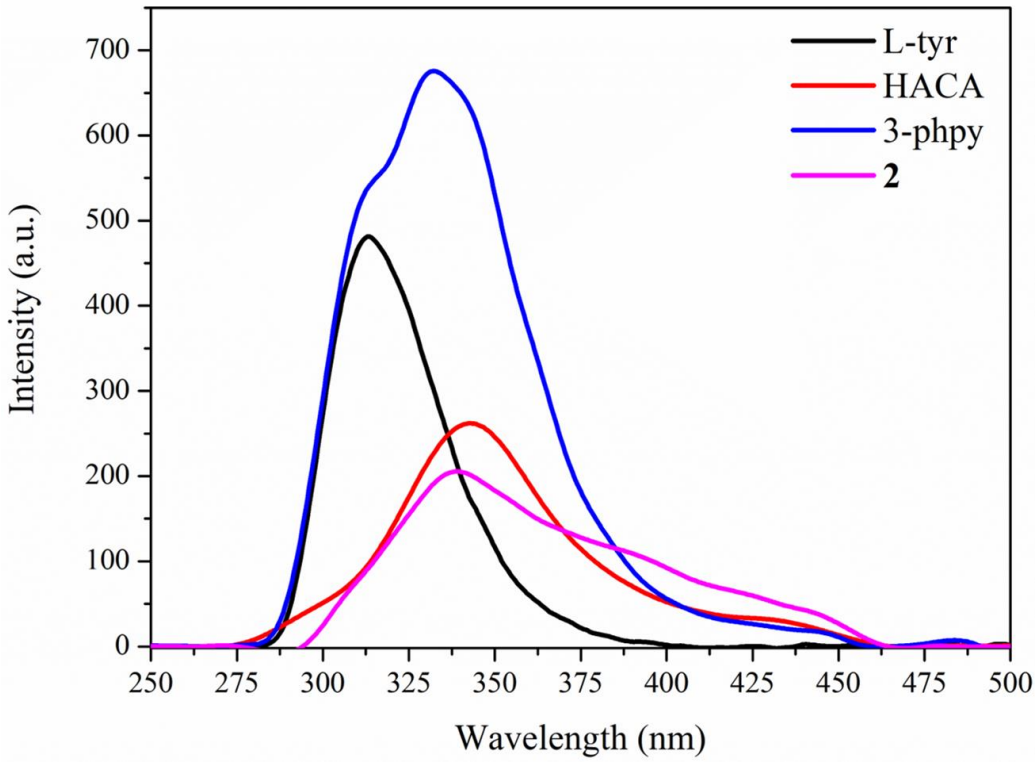

Figure S35. Emission spectra of compound **2**, HACA, 3-phpy and L-tyrosine, excited at 231 nm at 298K in Milli-Q water solution ($2.21 \cdot 10^{-6}$ M for L-tyrosine), MeOH solution ($1.61 \cdot 10^{-7}$ M for 3-phpy) or EtOH solutions ($2.50 \cdot 10^{-7}$ M for HACA and $4.05 \cdot 10^{-7}$ M for **2**).

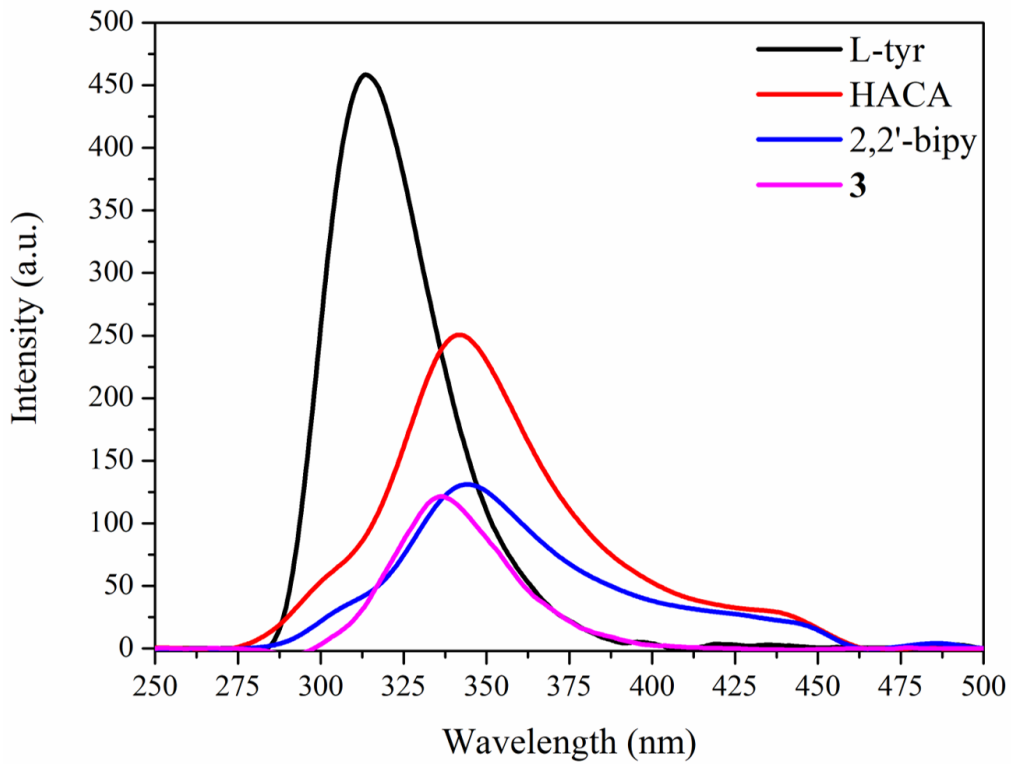

Figure S36. Emission spectra of compound **3**, HACA, 2,2'-bipy and L-tyrosine, excited at 232 nm at 298K in Milli-Q water solution ($2.21 \cdot 10^{-6}$ M for L-tyrosine), MeOH solution ($8.32 \cdot 10^{-6}$ M for 2,2'-bipy) or EtOH solutions ($2.50 \cdot 10^{-7}$ M for HACA and $5.24 \cdot 10^{-8}$ M for **3**).

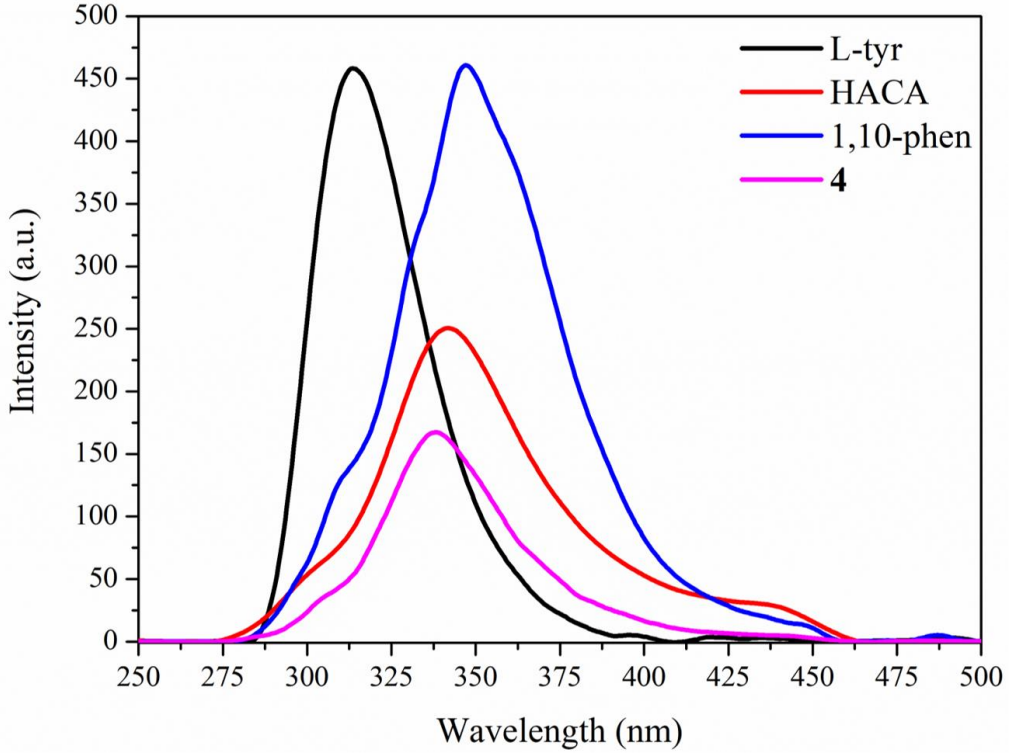

Figure S37. Emission spectra of compound **4**, HACA, 1,10-phen and L-tyrosine, excited at 232 nm at 298K in Milli-Q water solution ($2.21 \cdot 10^{-6}$ M for L-tyrosine), MeOH solution ($1.85 \cdot 10^{-7}$ M for 1,10-phen) or EtOH solutions ($2.50 \cdot 10^{-7}$ M for HACA and $1.50 \cdot 10^{-8}$ M for **4**).

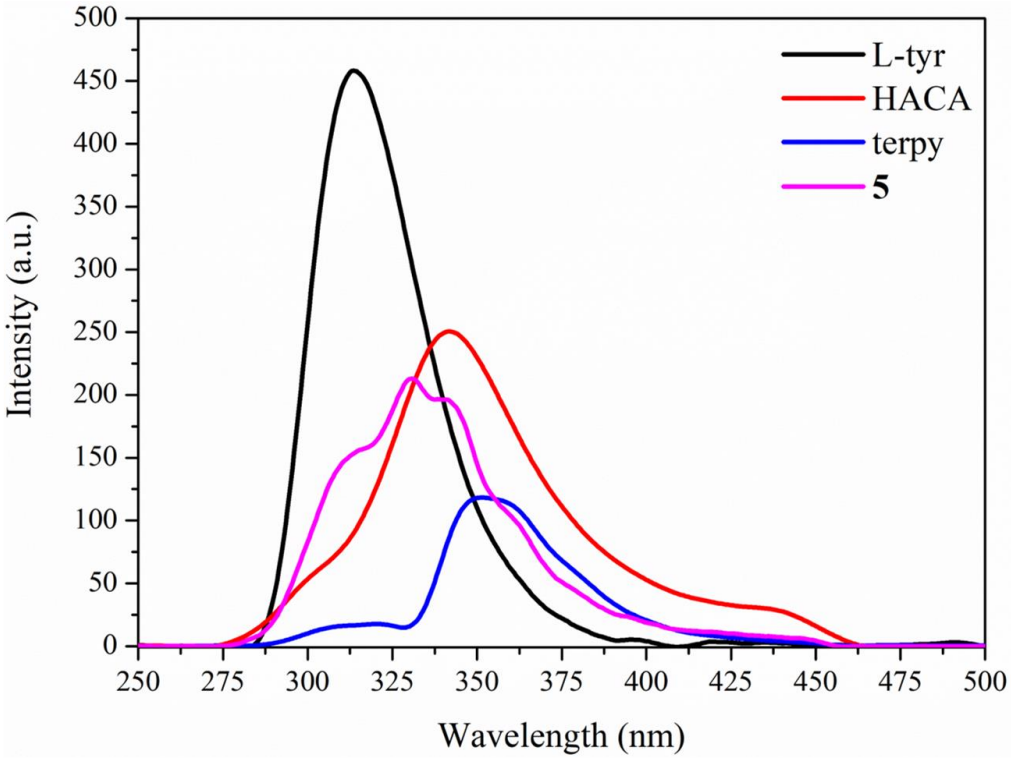

Figure S38. Emission spectra of compound **5**, HACA, terpy and L-tyrosine, excited at 232 nm at 298K in Milli-Q water solution ($2.21 \cdot 10^{-6}$ M for L-tyrosine), MeOH solution ($1.79 \cdot 10^{-8}$ M for terpy) or EtOH solutions ($2.50 \cdot 10^{-7}$ M for HACA and $7.39 \cdot 10^{-8}$ M for **5**).

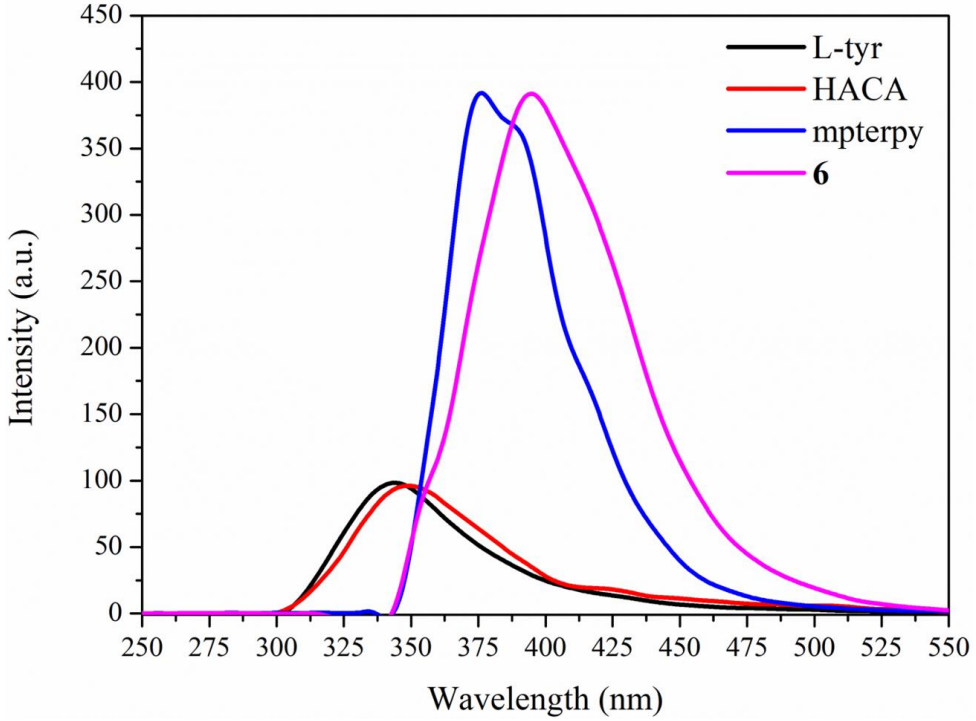

Figure S39. Emission spectra of compound **6**, HACA, mpterpy and L-tyrosine, excited at 294 nm at 298K in Milli-Q water solution ($2.21 \cdot 10^{-6}$ M for L-tyrosine) or EtOH solutions ($2.50 \cdot 10^{-7}$ M for HACA, $4.00 \cdot 10^{-9}$ M for mpterpy and $3.43 \cdot 10^{-8}$ M for **6**).

EXPERIMENTAL SECTION

Materials and General Methods

Zinc(II) acetate dihydrate ($Zn(OAc)_2 \cdot 2H_2O$), α-acetamidocinnamic acid (HACA), dPy = pyridine (py), 3-phenylpyridine (3-phpy), 2,2'-bipyridine (2,2'-bipy), 1,10-phenantroline monohydrate (1,10-phen·H_2O), 2,2′:6′,2″-terpyridine (terpy), 4′-(4-methylphenyl)-2,2′:6′,2″-terpyridine (mpterpy) ligands and ethanol (EtOH), methanol (MeOH), diethyl ether (Et_2O), dimethylformamide (DMF) and heptane as solvents were purchased from Sigma-Aldrich. Deuterated dimethylsulfoxide (dmso-d_6) was used for the NMR experiments and was purchased from Eurisotop (Saint-Aubin, France). All of them were used without further purification. All of the reactions and manipulations were carried out in air at room temperature (RT). Elemental analyses (C, H, N) were carried on a Thermo Scientific (Waltham, MA, USA) Flash 2000 CHNS Analyzer. FTIR-ATR spectra were recorded on a Perkin Elmer (Waltham, MA, USA) spectrometer, equipped with an attenuated total reflectance (ATR) accessory model MKII Golden Gate with diamond window in the range 4000–500 cm^{-1}. ^1H, $^{13}C\{^1H\}$ and DEPT-135 NMR spectra were recorded on an NMR-FT Bruker 360 (Karlsruhe, Germany) spectrometer in dmso-d_6 solution at RT. All of the chemical shifts (δ) are given in ppm relative to TMS as internal standard. The electronic spectra in EtOH solution for **1**-**6** and HACA, py and mpterpy ligands, in MeOH for 3-phpy, 2,2'-bipy, 1,10-phen and terpy ligands, and Milli-Q water for L-tyrosine were run on an Agilent HP 8453 UV-Vis spectrophotometer with a quartz cell having path length of 1 cm in the range of 190-500 nm. Fluorescence measurements were carried out with a Perkin Elmer LS 55 50 Hz Fluorescence Spectrometer using 1 cm quartz cell, in EtOH (**1**-**6**, HACA, py and mpterpy ligands), MeOH (3-phpy, 2,2'-bipy, 1,10-phen and terpy ligands) and Milli-Q water (L-tyrosine) solutions. The emission spectra were measured at 25 ºC. The samples were excited at their maximum emission wavelength and the emission were recorded between 200 and 600 nm. The data obtained were corrected by means of the Origin Pro 8.6 software.

Characterization of Compounds 1-6

$[Zn(\mu\text{-}O,O'\text{-}ACA)(ACA)(py)]_n$ (1). Yield: 174 mg (69% based on Zn). Elemental analysis calc(%). for $C_{27}H_{25}ZnN_3O_6$ (552.89): C 58.65; H 4.56; N 7.60; found: C 58.47; H 4.65; N 7.35. FTIR-ATR (wavenumber, cm^{-1}): 3239(m) [ν(N-H)], 3195-3059(br) [$\nu(C\text{-}H)_{ar}$] + [$\nu(C\text{-}H)_{alk}$], 2999-2809(br) [$\nu(C\text{-}H)_{al}$], 1658(w) [ν(C=O)], 1619(m), 1607(m)

[ν_{as}(COO)], 1569(m), 1548(m), 1527(m) [ν_{as}(COO)], 1490(m) [ν(C=C/C=N)], 1448(m), 1392(s) [ν_{s}(COO)], 1352(s) [δ(C=C/C=N)], 1312(m), 1293(m), 1219(w), 1209(w), 1137(w), 1070(w) [δ_{ip}(C-H)], 1046(w) [δ_{ip}(C-H)], 994(m) [δ_{ip}(C-H)], 935(w), 894(w), 847(w), 786(m), 770(s) [δ_{oop}(C-H)], 758(m) [δ_{oop}(C-H)], 690(s) [δ_{oop}(C-H)], 642(w), 622(m), 576(m), 568(m) 536(m), 526(m). ^{1}H NMR (360 MHz; dmso-d_6; Me_4Si; 298 K): δ = 9.23 [2H, s, NH_{ACA}], 8.65 [2H, d, ^{3}J = 5.8 Hz, *o*-H_{py}], 7.91 [1H, t, ^{3}J = 7.6 Hz, *p*-H_{py}], 7.51 [6H, m, *m*-H_{py} + *o*-H_{ACA}], 7.36 [4H, t, ^{3}J = 7.5 Hz, *m*-H_{ACA}], 7.29 [2H, d, ^{3}J = 7.2 Hz, *p*-H_{ACA}], 7.26 [2H, s, NH-C-CH_{ACA}], 1.96 [6H, s, CO-C$H_{3,ACA}$]. ^{13}C{^{1}H} NMR (360 MHz; dmso-d_6; Me_4Si; 298 K): δ = 170.54 [NH-*C*O_{ACA}], 168.39 [*C*OO_{ACA}], 149.49 [*o*-C_{py}], 137.57 [*p*-C_{py}], 135.04 [O_2C-C_{ACA}], 129.68 [HN-C-CH-C_{ACA}], 129.31 [*o*-C_{ACA}], 129.07 [*p*-C_{ACA}], 128.32 [*m*-C_{ACA}], 128.16 [NH-C-*C*H_{ACA}], 124.44 [*m*-C_{py}], 22.98 [CO-*C*$H_{3,ACA}$]. DEPT-135 NMR (360 MHz; dmso-d_6; Me_4Si; 298 K): δ = 149.46 [*o*-C_{py}], 137.75 [*p*-C_{py}], 129.31 [*o*-C_{ACA}], 129.14 [*p*-C_{ACA}], 128.35 [*m*-C_{ACA}], 128.21 [NH-C-*C*H_{ACA}], 124.52 [*m*-C_{py}], 22.96 [CO-*C*$H_{3,ACA}$]. UV-Vis: (EtOH, ~$1.15\cdot10^{-4}$–$1.06\cdot10^{-9}$ M) λ_{max} (log ε) = 201 nm (4.60), 278 nm (4.55). Fluorescence (EtOH, $3.54\cdot10^{-7}$ M): λ_{ex} = 234 nm; λ_{em} (Φ) = 338 nm (0.13).

[Zn(ACA)$_2$(3-phpy)$_2$]·EtOH (2). Yield: 171 mg (45% based on Zn). Elemental analysis calc(%). for $C_{46}H_{44}ZnN_4O_7$ (830.25): C 66.55; H 5.34; N 6.75; found: C 66.38; H 5.19; N 6.53. FTIR-ATR (wavenumber, cm^{-1}): 3476(br) [ν(O-H)], 3248(m), [ν(N-H)], 3178-3021(br) [ν(C-H)$_{ar}$] + [ν(C-H)$_{alk}$], 2978(w) [ν(C-H)$_{al}$], 1676(s) [ν(C=O)], 1646(w), 1590(s) [ν_{as}(COO)], 1509(m) [ν(C=C/C=N)], 1488(m), 1480(w), 1454(w), 1422(w), 1382(s) [ν_{s}(COO)], 1347(s) [δ(C=C/C=N)], 1270(m), 1206(w), 1158(w), 1141(w), 1112(w), 1072(w), 1049(w), 1032(w) [δ_{ip}(C-H)], 1012(w), 1000(w) [δ_{ip}(C-H)], 981(w), 962(w), 925(w), 898(w), 849(w), 818(w), 772(m), 759(s) [δ_{oop}(C-H)], 694(s) [δ_{oop}(C-H)], 657(m), 615(m), 586(w), 553(m), 522(s). ^{1}H NMR (360 MHz; dmso-d_6; Me_4Si; 298 K): δ = 9.29 [2H, s, NH_{ACA}], 8.90 [2H, s, *o*-H_{py}], 8.60 [2H, d, ^{3}J = 4.9 Hz, *o*-H_{py}], 8.14 [2H, d, ^{3}J = 7.9 Hz, *p*-H_{py}], 7.70 [4H, d, ^{3}J = 7.6 Hz, *o*-$H_{ph(3\text{-}phpy)}$],7.56 [2H, dd, ^{3}J = 8.1 Hz, 4.8 Hz, *m*-H_{py}], 7.50 [8H, m, *o*-H_{ACA} + *m*-$H_{ph(3\text{-}phpy)}$], 7.42 [2H, m, *p*-$H_{ph(3\text{-}phpy)}$], 7.34 [4H, t, ^{3}J = 7.4 Hz, *m*-H_{ACA}], 7.29 [2H, s, NH-C-CH_{ACA}], 7.27 [2H, s, *p*-H_{ACA}], 4.63 [0.2H, br, OH_{EtOH}], 3.43 [0.6H, q, ^{3}J = 7.1 Hz, C$H_{2,EtOH}$], 1.97 [6H, s, CO-C$H_{3,ACA}$], 1.04 [0.7H, t, ^{3}J = 7.1 Hz, C$H_{3,EtOH}$]. ^{13}C{^{1}H} NMR (360 MHz; dmso-d_6; Me_4Si; 298 K): δ = 170.67 [NH-*C*O_{ACA}], 168.48 [*C*OO_{ACA}], 148.42 [*o*-C_{py}], 147.60 [*o*-C_{py}], 136.80 [py-$C_{ph(3\text{-}phpy)}$], 135.98 [*m*-C_{py}], 135.12 [*p*-C_{py}], 135.05 [O_2C-C_{ACA}], 129.82 [HN-C-CH-C_{ACA}], 129.36

[*o*-C_{ACA}], 129.27 [*m*-$C_{ph(3\text{-}phpy)}$], 128.98 [*p*-C_{ACA}], 128.40 [*m*-C_{ACA}], 128.37 [*p*-$C_{ph(3\text{-}phpy)}$], 128.21 [NH-C-CH_{ACA}], 127.01 [*o*-$C_{ph(3\text{-}phpy)}$], 124.34 [*m*-CH_{py}], 56.11 [$CH_{2,EtOH}$], 23.02 [CO-$CH_{3,ACA}$], 18.63 [$CH_{3,EtOH}$]. DEPT-135 NMR (360 MHz; dmso-d_6; Me_4Si; 298 K): δ = 148.42 [*o*-C_{py}], 147.60 [*o*-C_{py}], 135.12 [*p*-C_{py}], 129.35 [*o*-C_{ACA}], 129.26 [*m*-$C_{ph(3\text{-}phpy)}$], 128.98 [*p*-C_{ACA}], 128.38 [*m*-C_{ACA}+*p*-$C_{ph(3\text{-}phpy)}$], 128.21 [NH-C-CH_{ACA}], 127.00 [*o*-$C_{ph(3\text{-}phpy)}$], 124.34 [*m*-CH_{py}], 56.11 [$CH_{2,EtOH}$], 23.02 [CO-$CH_{3,ACA}$], 18.62 [$CH_{3,EtOH}$]. UV-Vis: (EtOH, ~$4.71\cdot10^{-5}$–$1.01\cdot10^{-9}$ M) λ_{max} (log ε) = 202 nm (5.01), 273 nm (4.85). Fluorescence (EtOH, $4.05\cdot10^{-7}$ M): λ_{ex} = 231 nm; λ_{em} (Φ) = 339 nm (0.065).

[Zn(ACA)$_2$(2,2'-bipy)]·4EtOH (3). Yield: 202 mg (55% based on Zn). Elemental analysis calc(%). for $C_{40}H_{52}ZnN_4O_{10}$ (814.25): C 59.00; H 6.44; N 6.88; found: C 58.74; H 6.32; N 6.57. FTIR-ATR (wavenumber, cm^{-1}): 3640-3370(br) [ν(O-H)], 3216(br) [ν(N-H)], 3152-3008(br) [$\nu(C\text{-}H)_{ar}$] + [$\nu(C\text{-}H)_{alk}$], 2803(w) [$\nu(C\text{-}H)_{al}$], 1664(w) [ν(C=O)], 1642(w), 1598(w), 1579(w), 1564(m), 1523(m) [ν_{as}(COO)], 1492(m) [ν(C=C/C=N)], 1444(w), 1415(s) [ν_s(COO)], 1370(m) [δ(C=C/C=N)], 1344(w), 1319(w), 1291(w), 1255(w), 1212(w), 1180(w) 1155(w) 1106(w) 1080(w), 1060(w), 1031(w) [δ_{ip}(C-H)], 984(w), 938(w), 898(w), 850(w), 767(s) [δ_{oop}(C-H)], 734(m), 694(s) [δ_{oop}(C-H)], 655(m), 627(w), 609(m), 593(m), 565(m), 547(w), 522(s). ^{1}H NMR (360 MHz; dmso-d_6; Me_4Si; 298 K): δ = 9.14 [2H, s, NH_{ACA}], 8.82 [2H, d, ^{3}J = 3.5 Hz, *o*-H_{py}], 8.60 [2H, d, ^{3}J = 8.4 Hz, *m*-H_{py}], 8.21 [2H, m, *p*-H_{py}], 7.72 [2H, br, *m*-H_{py}], 7.47 [4H, d, ^{3}J = 7.7 Hz, *o*-H_{ACA}], 7.33 [4H, t, ^{3}J = 7.6 Hz, *m*-H_{ACA}], 7.27 [2H, d, ^{3}J = 7.2 Hz, *p*-H_{ACA}], 7.23 [2H, s, NH-C-CH_{ACA}], 4.39 [0.2H, s, O$H_{,EtOH}$], 1.93 [6H, s, CO-C$H_{3,ACA}$], 1.06 [0.6H, t, ^{3}J = 7.1 Hz, C$H_{3,EtOH}$]. ^{13}C{^{1}H} NMR (360 MHz; dmso-d_6; Me_4Si; 298 K): δ = 170.61 [NH-*C*O$_{ACA}$], 168.24 [*C*OO$_{ACA}$], 149.18 [*o*-CH_{py}], 140.40 [*o*-C_{py}], 140.20 [*p*-C_{py}], 135.18 [O_2C-*C*$_{ACA}$], 129.69 [HN-C-CH-*C*$_{ACA}$], 129.30 [*o*-*C*$_{ACA}$], 128.58 [*p*-*C*$_{ACA}$], 128.30 [*m*-*C*$_{ACA}$], 128.09 [NH-C-*C*H$_{ACA}$], 126.26 [*m*-C_{py}], 121.75 [*m*-C_{py}], 23.06 [CO-*C*H$_{3,ACA}$]. DEPT-135 NMR (360 MHz; dmso-d_6; Me_4Si, 298 K): δ = 149.18 [*o*-*C*H$_{py}$], 129.30 [*o*-*C*$_{ACA}$], 128.58 [*p*-*C*$_{ACA}$], 128.30 [*m*-*C*$_{ACA}$], 128.08 [NH-C-*C*H$_{ACA}$], 126.27 [*m*-C_{py}], 121.75 [*m*-C_{py}], 23.05 [CO-*C*H$_{3,ACA}$]. UV-Vis: (EtOH, ~$5.90\cdot10^{-5}$–$7.86\cdot10^{-10}$ M) λ_{max} (log ε) = 202 nm (4.97), 244 nm (4.69), 280 nm (4.92). Fluorescence (EtOH, $5.24\cdot10^{-8}$ M): λ_{ex} = 232 nm; λ_{em} (Φ) = 336 nm (0.023).

[Zn(ACA)$_2$(1,10-phen)][Zn(ACA)$_2$(1,10-phen)]·3EtOH (4). Yield: 232 mg (70% based on Zn). Elemental analysis calc(%). for $C_{74}H_{74}Zn_2N_8O_{15}$ (1446.20): C 61.46; H 5.16; N 7.75; found: C 61.35; H 5.02; N 7.59. FTIR-ATR (wavenumber, cm^{-1}): 3387(w)

[ν(O-H)], 3215(w) [ν(N-H)], 3153-3060(br) [ν(C-H)$_{ar}$] + [ν(C-H)$_{alk}$], 2998-2946(br) [ν(C-H)$_{al}$], 1675(w) [ν(C=O)], 1642(w), 1567(m) [ν_{as}(COO)], 1518(m) [ν_{as}(COO)], 1489(m) [ν(C=C/C=N)], 1449(w), 1424(sh), 1405(s) [ν_{s}(COO)], 1365(m) [ν_{s}(COO)], 1343(sh) [δ(C=C/C=N)], 1277(w), 1219(w), 1143(w), 1106(w) [δ_{ip}(C-H)], 1082(w), 1050(w), 1030(w), 1002(w), 981(w), 963(w), 900(w), 871(w), 846(w), 797(w), 772(s) [δ_{oop}(C-H)], 724(s) [δ_{oop}(C-H)], 693(s) [δ_{oop}(C-H)], 646(w), 623(w), 593(m), 560(w), 543(m), 525(w). ^{1}H NMR (360 MHz; dmso-d_6; Me$_4$Si; 298 K): δ = 9.15 [2H, s, NH_{ACA}], 9.10 [2H, s, *o*-H_{py}], 8.86 [2H, d, ^{3}J = 8.2 Hz, *p*-H_{py}], 8.22 [2H, s, $H_{ph(1,10\text{-}phen)}$], 8.08 [2H, dd, ^{3}J = 8.2 Hz, 4.9 Hz, *m*-H_{py}], 7.43 [4H, d, ^{3}J = 7.9 Hz, *o*-H_{ACA}], 7.31 [4H, t, ^{3}J = 7.6 Hz, *m*-H_{ACA}], 7.24 [2H, d, ^{3}J = 7.2 Hz, *p*-H_{ACA}], 7.20 [2H, s, NH-C-CH_{ACA}], 4.40 [0.2H, s, OH_{EtOH}], 1.90 [6H, s, CO-C$H_{3,ACA}$], 1.05 [0.7H, t, ^{3}J = 7.0 Hz, C$H_{3,EtOH}$]. ^{13}C{^{1}H} NMR (360 MHz; dmso-d_6; Me$_4$Si; 298 K): δ = 170.40 [NH-*C*O$_{ACA}$], 168.06 [*C*OO$_{ACA}$], 149.66 [*o*-*C*H$_{py}$], 140.15 [*o*-*C*$_{py}$], 139.63 [*p*-*C*$_{py}$], 135.33 [O$_2$C-*C*$_{ACA}$], 130.04 [HN-C-CH-*C*$_{ACA}$], 129.23 [*o*-*C*$_{ACA}$+*p*-*C*$_{ACA}$], 128.49 [*m*-*C*$_{py}$], 128.23 [*m*-*C*$_{ACA}$], 127.92 [NH-C-*C*H$_{ACA}$], 126.99 [*C*H$_{ph(1,10\text{-}phen)}$], 125.59 [*m*-*C*H$_{py}$], 56.10 [*C*H$_{2,EtOH}$], 23.08 [CO-*C*H$_{3,ACA}$], 18.62 [*C*H$_{3,EtOH}$]. DEPT-135 NMR (360 MHz; dmso-d_6; Me$_4$Si, 298 K): δ = 149.66 [*o*-*C*H$_{py}$], 139.63 [*p*-*C*$_{py}$], 129.24 [*o*-*C*$_{ACA}$+*p*-*C*$_{ACA}$], 128.24 [*m*-*C*$_{ACA}$], 127.92 [NH-C-*C*H$_{ACA}$], 126.99 [*C*H$_{ph(1,10\text{-}phen)}$], 125.50 [*m*-*C*H$_{py}$], 23.09 [CO-*C*H$_{3,ACA}$]. UV-Vis: (EtOH, ~$2.74\cdot10^{-5}$–$4.50\cdot10^{-10}$ M) λ_{max} (log ε) = 201 nm (5.19), 271 nm (5.31). Fluorescence (EtOH, $1.50\cdot10^{-8}$ M): λ_{ex} = 232 nm; λ_{em} (Φ) = 338 nm (0.029).

[Zn(ACA)$_2$(terpy)]·2DMF (5). Yield: 169 mg (59% based on Zn). Elemental analysis calc(%). for C$_{43}$H$_{45}$ZnN$_7$O$_8$ (629.98): C 60.53; H 5.32; N 11.49; found: C 60.42; H 5.17; N 11.24. FTIR-ATR (wavenumber, cm^{-1}): 3309(m) [ν(N-H)], 3191-3024(br) [ν(C-H)$_{ar}$] + [ν(C-H)$_{alk}$], 2998-2862(br) [ν(C-H)$_{al}$], 1669(br) [ν(C=O)]$_{ACA+DMF}$, 1610(s), 1594(s) [ν_{as}(COO)], 1509(w) [ν(C=C/C=N)], 1490(w), 1451(w), 1440(w), 1408(w), 1372(s) [ν_{s}(COO)], 1335(m) [δ(C=C/C=N)], 1319(m), 1267(m), 1257(w) 1211(w), 1200(w), 1166(w), 1132(w), 1098(m) [δ_{ip}(C-H)], 1063(w), 1046(w), 1023(w), 1015(w) [δ_{ip}(C-H)], 1001(w), 975(w), 930(w), 887(w), 845(w), 836(w), 785(s) [δ_{oop}(C-H)], 770(s) [δ_{oop}(C-H)], 729(m), 699(m), 662(s), 651(m), 639(w), 604(w), 573(s), 520(w), 513(w). ^{1}H NMR (360 MHz; dmso-d_6; Me$_4$Si; 298 K): δ = 8.96 [2H, s, NH_{ACA}], 8.87 [2H, d, ^{3}J = 4.1 Hz, *o*-$H_{py\text{-}side}$], 8.79 [2H, d, ^{3}J = 7.9 Hz, *m*-$H_{py\text{-}side}$], 8.71 [2H, d, ^{3}J = 8.0 Hz, *m*-$H_{py\text{-}center}$], 8.54 [1H, t, ^{3}J = 7.5 Hz, *p*-$H_{py\text{-}center}$], 8.27 [2H, t, ^{3}J = 7.5 Hz, *p*-$H_{py\text{-}side}$], 7.79 [2H, br, *m*-$H_{py\text{-}side}$], 7.38 [4H, br, *o*-H_{ACA}], 7.29 [4H, t, ^{3}J = 7.2 Hz, *m*-H_{ACA}], 7.23 [2H, d, ^{3}J = 7.0 Hz, *p*-

H$_{ACA}$], 7.10 [2H, s, NH-C-C*H*$_{ACA}$], 1.84 [6H, s, CO-C*H*$_{3,ACA}$]. ^{13}C{^{1}H} NMR (360 MHz; dmso-d_6; Me$_4$Si; 298 K): δ = 169.33 [NH-*C*O$_{ACA}$], 167.87 [*C*OO$_{ACA}$], 149.25 [*o*-*C*H$_{py\text{-}side}$], 148.34 [*o*-*C*$_{py\text{-}center}$], 147.71 [*o*-*C*$_{py\text{-}side}$], 142.88 [*p*-*C*$_{py\text{-}center}$], 140.50 [*p*-*C*$_{py\text{-}side}$], 135.39 [O$_2$C-*C*$_{ACA}$], 129.13 [HN-C-CH-*C*$_{ACA}$+*o*-*C*$_{ACA}$], 128.17 [*p*-*C*$_{ACA}$], 127.75 [*m*-*C*$_{ACA}$], 127.18 [NH-C-*C*H$_{ACA}$], 126.93 [*m*-*C*$_{py\text{-}side}$], 122.60 [*m*-*C*$_{py\text{-}side}$], 122.14 [*m*-*C*$_{py\text{-}center}$], 23.04 [CO-*C*H$_{3,ACA}$]. DEPT-135 NMR (360 MHz; dmso-d_6; Me$_4$Si, 298 K): δ = 149.25 [*o*-*C*H$_{py\text{-}side}$], 142.87 [*p*-*C*$_{py\text{-}center}$], 140.50 [*p*-*C*$_{py\text{-}side}$], 129.12 [*o*-*C*$_{ACA}$], 128.16 [*p*-*C*$_{ACA}$], 127.75 [*m*-*C*$_{ACA}$], 127.22 [NH-C-*C*H$_{ACA}$], 126.92 [*m*-*C*$_{py\text{-}side}$], 122.60 [*m*-*C*$_{py\text{-}side}$], 122.13 [*m*-*C*$_{py\text{-}center}$], 23.04 [CO-*C*H$_{3,ACA}$]. UV-Vis: (EtOH, ~$7.10\cdot10^{-5}$–$8.67\cdot10^{-9}$ M) λ_{max} (log ε) = 201 nm (4.89), 272 nm (4.83). Fluorescence (EtOH, $7.39\cdot10^{-8}$ M): λ_{ex} = 232 nm; λ_{em} (Φ) = 331 nm (0.058).

[Zn(ACA)$_2$(mpterpy)]·4MeOH (6). Yield: 312 mg (74% based on Zn). Elemental analysis calc(%). For $C_{48}H_{53}ZnN_5O_{10}$ (925.35): C 62.30; H 5.77; N 7.57; found: C 62.15; H 5.54; N 7.38. FTIR-ATR (wavenumber, cm^{-1}): 3590-3373(br) [ν(O-H)], 3231 [ν(N-H)], 3108-3027(br) [ν(C-H)$_{ar}$] + [ν(C-H)$_{alk}$], 2983-2865(br) [ν(C-H)$_{al}$], 1672(w) [ν(C=O)], 1647(w), 1596(s) [ν$_{as}$(COO)], 1552(m), 1524(w), 1479(m) [ν(C=C/C=N)], 1446(w), 1426(w), 1367(s) [ν$_s$(COO)], 1339(s) [δ(C=C/C=N)], 1255(m), 1205(w), 1166(w), 1132(w), 1071(w), 1024(m) [δ$_{ip}$(C-H)], 1014(m) [δ$_{ip}$(C-H)], 975(w), 928(w), 894(w), 844(w), 821(w), 790(s) [δ$_{oop}$(C-H)], 748(m), 730(m), 692(s) [δ$_{oop}$(C-H)], 659(m), 637(m), 605(m), 571(m), 526(m). ^{1}H NMR (360 MHz; dmso-d_6; Me$_4$Si; 298 K): δ = 9.01 [2H, s, N*H*$_{ACA}$], 8.97 [2H, s, *m*-*H*$_{py\text{-}center}$], 8.88 [4H, m, (*o*+*m*)-*H*$_{py\text{-}side}$], 8.25 [2H, t, ^{3}J = 7.9 Hz, *m*-*H*$_{py\text{-}side}$], 8.17 [2H, d, ^{3}J = 7.9 Hz, *o*-*H*$_{ph(mpterpy)}$], 7.78 [2H, m, *p*-*H*$_{py\text{-}side}$], 7.42 [6H, m, *o*-*H*$_{ACA}$+ *m*-*H*$_{ph(mpterpy)}$], 7.30 [4H, t, ^{3}J = 7.1 Hz, *m*-*H*$_{ACA}$], 7.22 [2H, m, *p*-*H*$_{ACA}$], 7.12 [2H, s, NH-C-C*H*$_{ACA}$], 2.44 [3H, s, C*H*$_{3,mpterpy}$], 1.85 [6H, s, CO-C*H*$_{3,ACA}$]. ^{13}C{^{1}H} NMR (360 MHz; dmso-d_6; Me$_4$Si; 298 K): δ = 169.18 [NH-*C*O$_{ACA}$], 167.85 [*C*OO$_{ACA}$], 153.05 [*o*-*C*$_{py\text{-}center}$], 148.89 [*o*-*C*H$_{py\text{-}side}$], 148.80 [*o*-*C*$_{py\text{-}side}$], 147.78 [*p*-*C*$_{py\text{-}center}$], 140.52 [H$_3$C-C-C-C-*C*$_{mpterpy}$], 139.98 [*p*-*C*$_{py\text{-}side}$], 135.42 [O$_2$C-*C*$_{ACA}$], 132.26 [*p*-*C*$_{ph(mpterpy)}$], 130.54 [HN-C-CH-*C*$_{ACA}$], 129.70 [*o*-*C*$_{ACA}$], 129.10 [*p*-*C*$_{ACA}$], 128.14 [*m*-*C*$_{ACA}$], 127.60 [NH-C-*C*H$_{ACA}$+ *m*-*C*$_{ph(mpterpy)}$], 127.00 [*o*-*C*$_{ph(mpterpy)}$], 126.55 [*m*-*C*$_{py\text{-}side}$], 122.25 [*m*-*C*$_{py\text{-}side}$], 118.89 [*m*-*C*$_{py\text{-}center}$], 23.02 [CO-*C*H$_{3,ACA}$], 20.95 [*C*H$_{3,mpterpy}$]. DEPT-135 NMR (360 MHz; dmso-d_6; Me$_4$Si, 298 K): δ = 148.89 [*o*-*C*H$_{py\text{-}side}$], 139.97 [*p*-*C*$_{py\text{-}side}$], 129.70 [*o*-*C*$_{ACA}$], 129.09 [*p*-*C*$_{ACA}$], 128.13 [*m*-*C*$_{ACA}$], 127.59 [NH-C-*C*H$_{ACA}$+ *m*-*C*$_{ph(mpterpy)}$], 126.98 [*o*-*C*$_{ph(mpterpy)}$], 126.54 [*m*-*C*$_{py\text{-}side}$], 122.24 [*m*-*C*$_{py\text{-}side}$], 118.88 [*m*-*C*$_{py\text{-}center}$], 23.02 [CO-

C$H_{3,ACA}$], 20.95 [*C*$H_{3,mpterpy}$]. UV-Vis: (EtOH, ~$3.43\cdot10^{-5}$–$8.75\cdot10^{-9}$ M) λ_{max} (log ε) = 201 nm (4.99), 279 nm (5.00). Fluorescence (EtOH, $3.43\cdot10^{-8}$ M): λ_{ex} = 294 nm; λ_{em} (Φ) = 395 nm (0.038).

X-ray Crystallographic Refinement Data

The X-ray intensity data were measured on a D8 Venture system equipped with a multilayer monochromate and a Mo microfocus (λ = 0.71073 Å). For **1**, the integration of the data using a monoclinic unit cell yielded a total of 7618 reflections to a maximum θ angle of 30.59° (0.70 Å resolution), of which 7618 were independent (average redundancy 1.000, completeness = 99.4%, R_{int} = 4.77%, R_{sig} = 3.44%) and 6307 (82.79%) were greater than $2\sigma(F^2)$. The calculated minimum and maximum transmission coefficients (based on crystal size) are 0.6269 and 0.7461. For **2**, the integration of the data using a monoclinic unit cell yielded a total of 37250 reflections to a maximum θ angle of 30.56° (0.70 Å), of which 6212 were independent (average redundancy 5.996, completeness = 99.4%, R_{int} = 6.67%, R_{sig} = 4.97%) and 4682 (75.37%) were greater than $2\sigma(F^2)$. The calculated minimum and maximum transmission coefficients (based on crystal size) are 0.6814 and 0.7461. For **3**, the integration of the data using a monoclinic unit cell yielded a total of 52003 reflections to a maximum θ angle of 26.50° (0.80 Å), of which 8520 were independent (average redundancy 6.104, completeness = 99.4%, R_{int} = 12.37%, R_{sig} = 7.85%) and 5690 (66.78%) were greater than $2\sigma(F^2)$. The calculated minimum and maximum transmission coefficients (based on crystal size) are 0.5569 and 0.7454. For **4**, the integration of the data using an orthorhombic unit cell yielded a total of 66762 reflections to a maximum θ angle of 30.06° (0.71 Å resolution), of which 19837 were independent (average redundancy 3.366, completeness = 99.9%, R_{int} = 13.00%, R_{sig} = 14.88%) and 9892 (49.87%) were greater than $2\sigma(F^2)$. The calculated minimum and maximum transmission coefficients (based on crystal size) are 0.6580 and 0.7448. For **5**, the integration of the data using a monoclinic unit cell yielded a total of 45954 reflections to a maximum θ angle of 30.62° (0.70 Å resolution), of which 6337 were independent (average redundancy 7.252, completeness = 99.2%, R_{int} = 10.01%, R_{sig} = 6.99%) and 4298 (67.82%) were greater than $2\sigma(F^2)$. The calculated minimum and maximum transmission coefficients (based on crystal size) are 0.6052 and 0.7461. For **6**, the integration of the data using a triclinic unit cell yielded a total of 66736 reflections to a maximum θ angle of 30.66° (0.70 Å resolution), of which 14116 were independent (average redundancy 4.728, completeness = 99.0%, R_{int} = 7.74%, R_{sig} = 6.64%) and 9664

(68.46%) were greater than $2\sigma(F^2)$. The calculated minimum and maximum transmission coefficients (based on crystal size) are 0.6182 and 0.7461.

The structures were solved and refined using a SHELX (version 2018/3).[1] For **1**, the final anisotropic full-matrix least-squares refinement on $|F|^2$ with 306 variables converged at R_1 = 5.59%, for the observed data and wR_2 = 15.21% for all data. For **2**, the final anisotropic full-matrix least squares refinement on $|F|^2$ with 265 variables converged at R_1 = 6.01% for the observed data and wR_2 = 14.99% for all data. For **3**, the final anisotropic full-matrix least squares refinement on $|F|^2$ with 503 variables converged at R_1 = 5.64% for the observed data and wR_2 = 16.00% for all data. For **4**, the final anisotropic full-matrix least squares refinement on $|F|^2$ with 899 variables converged at R_1 = 4.15% for the observed data and wR_2 = 10.85% for all data. For **5**, the final anisotropic full-matrix least squares refinement on $|F|^2$ with 315 variables converged at R_1 = 7.63%, for the observed data and wR_2 = 17.01% for all data. For **6**, the final anisotropic full-matrix least-squares refinement on $|F|^2$ with 586 variables converged at R_1 = 6.31%, for the observed data and wR_2 = 18.49% for all data.

For **1**-**6** the final cell constants and volume are based upon the refinement of the XYZ-centroids of reflections above 2θ $\sigma(I)$. Data were corrected for absorption effects using the Multi-Scan method (SADABS). Molecular graphics were generated using Mercury 4.3.1 software,[2,3] using the POV-Ray image package.[4] The color codes for all the molecular graphics except **4** are as follows: dark blue (Zn), red (O), light blue (N), dark gray (C), and white (H). For **4**, the colors dark green (**4a**) and blue (**4b**) have been used for distinguishing the two different Zn(II) atoms and the rest of the atoms have been represented following the same color codes as in the previous complexes.

References

1 G. M. Sheldrick, *Acta Cryst.*, 2008, **A64**, 112‑122.

2 C. F. Macrae, P. R. Edgington, P. McCabe, E. Pidcock, G. P. Shields, R. Taylor, M. Towler and J. van de Streek, *J. Appl. Cryst.*, 2006, **39**, 453–457.

3 C. F. Macrae, I. J. Bruno, J. A. Chisholm, P. R. Edgington, P. McCabe, E. Pidcock, L. Rodriguez-Monge, R. Taylor, J. van de Streek and P. A. Wood, *J. Appl. Cryst.*, 2008, **41**, 466–470.

4 Persistence of Vision Pty. Ltd. Persistence of Vision (TM) Raytracer; Persistence of Vision Pty. Ltd.: Williamstown, Australia, 2004.